KfK 4265
Mai 1987

Corrosion Behaviour of Container Materials for the Disposal of High-Level Waste Forms in Rock Salt Formations

E. Smailos, W. Schwarzkopf, R. Köster
Institut für Nukleare Entsorgungstechnik

Kernforschungszentrum Karlsruhe

KERNFORSCHUNGSZENTRUM KARLSRUHE

Institut für Nukleare Entsorgungstechnik

KfK 4265

Corrosion behaviour of container materials for the disposal of high-level waste forms in rock salt formations

E. Smailos, W. Schwarzkopf, R. Köster

Kernforschungszentrum Karlsruhe GmbH, Karlsruhe

Kernforschungszentrum Karlsruhe GmbH
Postfach 3640, 7500 Karlsruhe 1

ISSN 0303-4003

Summary

In safety analyses for a repository in rock salt an ingress of brines during the post-operational phase is postulated and the consequences are analysed. To provide an additional protection of HLW forms against radionuclide mobilization by attack of corrosive salt brines, the possibility of using a corrosion resistant packaging as a barrier during the high temperature phase in the repository (some 10^2 years) is being investigated in KfK.

In 1983-1984 extensive laboratory-scale experiments (immersion tests) to evaluate the long-term corrosion behaviour of selected materials in brines and first in situ experiments were performed. In the laboratory experiments the materials Ti 99.8-Pd, Hastelloy C4 and hot-rolled low carbon steel (reference materials in the joint European corrosion programme) as well cast steel, spheroidal cast iron, Si-cast iron and the Ni-Resists type D2 and D4 were investigated. The investigated parameters were: temperature (90°C, 170°C, 200°C), gamma-radiation (10^5 rad/h, 90°C) and different compositions of salt brines. In addition, first investigations were conducted to the influence of manufacturing induced material differences on corrosion.

According to the long-term studies carried out until now, Ti 99.8-Pd exhibits the highest corrosion resistance. After testing of about 600 days this material corroded at a very low corrosion rate (<1 µm/a) both with and without gamma-irradiation and has so far proved resistant to local corrosion and stress corrosion cracking. Hastelloy C4 has also resisted pitting corrosion and stress corrosion cracking, in the absence of irradiation, and its corrosion rate has been low at all testing temperatures (<1 µm/a), but it has been attacked by crevice corrosion. When it was exposed to irradiation, considerable pitting corrosion was observed in addition to crevice corrosion and an increase in the corrosion rate. The two steels (fine-grained structural steel, cast steel) were unaffected by pitting, crevice corrosion and stress corrosion cracking. They corroded in the absence of irradiation uniformly at a high rate (e.g.

100 µm/a at 170°C) which, however, is still acceptable for a thick-walled container. Under gamma-irradiation their corrosion rates greatly increased and the corrosion attack was non-uniformly with shallow pit formation. Spheroidal cast iron, Sicast iron and the 2 Ni-Resists were attacked by pitting corrosion and/ or intergranular corrosion, hence, they are not suitable as materials for long-term resistant HLW packagings.

The available corrosion results show that, in addition to Ti 99.8-Pd, also Hastelloy C4 and unalloyed steels are suitable in principle for the development of long-term stability HLW-containers, if the gamma dose rate is reduced by suitable shielding. Furthermore, the susceptibility of Hastelloy C4 to crevice corrosion must be taken on account. Further studies will be necessary to provide final evidence of the suitability of the materials examined. These will mainly involve clarification of questions related to hydrogen embrittlement (Ti 99.8-Pd, unalloyed steels) and to the influence of specimen-surface to medium-volumen ratio, pressure and saline impurities (e.g. J^-, Br^-) on corrosion. Such investigations are in progress.

Untersuchungen zum Korrosionsverhalten von Behältermaterialien für die Endlagerung von hochradioaktiven Abfallprodukten in Steinsalzformationen

Zusammenfassung

Im Rahmen von Störfallbetrachtungen für ein Endlager in einer Steinsalzformation wird das Zufließen von Salzlösungen zu den Abfällen unterstellt. Zum Schutz der hochradioaktiven Abfallprodukte (HAW-Produkte) gegen eine Radionuklid-Mobilisierung beim Angriff solcher korrosiven Salzlösungen wird die Möglichkeit der Verwendung einer korrosionsresistenten Verpackung als Barriere während der Hochtemperaturphase im Endlager (einige 10^2 Jahre) untersucht.

Hier wird über Ergebnisse weitergehender Laboruntersuchungen (Immersionsversuche) zum Langzeit-Korrosionsverhalten vorausgewählter Werkstoffe sowie über erste in situ-Korrosionsexperimente berichtet. In den Laborexperimenten wurden neben den aussichtsreichsten Werkstoffen Ti 99,8-Pd, Hastelloy C4 und Feinkornbaustahl (Referenzwerkstoffe des europäischen Korrosionsprogramms) zusätzlich Stahlguß, Sphäroguß, Si-Guß und die beiden Ni-Resiste Typ D2 und Typ D4 untersucht. Die Prüfung der Werkstoffe erfolgte in verschiedenen Salzlösungen unter den Parametern Temperatur (90°C, 170°C, 200°C), Gamma-Strahlung (10^5rad/h, 90°C) und Zusammensetzung der Korrosionsmedien.

Die bisherigen Langzeituntersuchungen zeigen, daß Ti 99,8-Pd die höchste Korrosionsresistenz aufweist. Nach der bisherigen Prüfzeit von ca. 600 Tagen korrodierte dieser Werkstoff mit und ohne Gamma-Bestrahlung mit einer sehr niedrigen Rate ($\leq$ 0,7 µm/a) und war bisher beständig gegenüber Lokal- und Spannungsrißkorrosion. Hastelloy C4 blieb ebenfalls ohne Bestrahlung auch nach langen Prüfzeiten beständig gegenüber Loch- und Spannungsrißkorrosion und seine Korrosionsrate war gering ($\leq$ 0,3 µm/a), jedoch wurde er durch Spaltkorrosion angegriffen. Unter Bestrahlung trat neben Spaltkorrosion und einer Erhöhung seiner Korrosionsrate zusätzlich starker Lochfraß auf. Die beiden Stähle (Feinkornbaustahl, Stahlguß) korrodierten ohne Bestrahlung weitgehend gleichmäßig mit einer hohen, jedoch für einen dickwandigen Behälter akzeptablen Korrosionsrate (z.B. 100 µm/a bei 170°C). Unter hoher Gamma-Bestrahlung von 10^5rad/h nahm ihre Korrosionsrate stark zu und der Korrosionsangriff erfolgte ungleichmäßig unter Muldenbildung.

Sphäroguß, Si-Guß und die beiden Ni-Resiste wurden durch Loch- und/oder interkristalline Korrosion angegriffen und sind damit als Werkstoffe für langzeitbeständige HAW-Behälter ungeeignet.

Die bisher vorliegenden Korrosionsergebnisse zeigen, daß außer Ti 99,8-Pd auch Hastelloy C4 und unlegierte Stähle prinzipiell für die Realisierung von langzeitbeständigen HAW-Behältern geeignet sind, wenn die Gamma-Dosisleistung durch eine geeignete Abschirmung bzw. dickwandige Behälterkonstruktion reduziert wird und bei Hastelloy C4-Behältern enge Spalten vermieden werden. Zum endgültigen Nachweis der Eignung der oben genannten Werkstoffe sind weitere Untersuchungen notwendig. Sie betreffen hauptsächlich die Klärung der Fragen der H_2-Versprödung (Ti 99,8-Pd, unlegierte Stähle) sowie des Einflusses der Gamma-Dosisleistung und der Salzverunreinigungen (z.B. J^-, Br^-) auf die Korrosion.

Table of contents

1. Introduction

According to the current waste management concept of the Federal Republic of Germany the high level wastes (HLW) shall be incorporated in borosilicate glass, encapsulated in a Cr-Ni-steel canister and disposed of in a rock salt repository. In safety analyses for the post-operational phase an ingress of brines into the repository is postulated and the consequences are analysed. As a result of this accident event the HLW might get in contact with corrosive salt brines, since a long-term resistance of the Cr-Ni-steel canisters particulary due to its susceptibility to stress corrosion cracking /1/ cannot be expected in chloride containing aqueous solutions.

To provide an additional protection of HLW forms against radionuclide mobilization by attack of corrosive brines, the possibility of using the HLW packaging as a barrier during the high temperature phase (some 10^2 years) in the repository is being investigated. For this purpose packaging materials are required having sufficient structural strength and in particular a high corrosion resistance in $MgCl_2$-rich brines.

A possible packaging concept for HLW forms with barrier function in the repository is the use of a double-walled metallic packaging. In this case the Cr-Ni-steel canister containing the HLW form as provided in the German concept is surrounded by an additional corrosion resistant container.

In order to determine corrosion resistant container materials, investigations are performed at KfK in the past years on a number of preselected materials. The results of previous screening tests and first detailed corrosion studies on unalloyed steels, Cr-Ni-steels, cast materials, nickel base alloys and the titanium base alloy Ti 99.8-Pd in salt brines have been reported elsewhere /1,2,3,4,5,6/. From the results of these studies the following eight materials were selected for long-term corrosion experiments:

- Ti 99.8-Pd (DIN-No. 3.7025.10),
- Hastelloy C 4 (DIN-No. 2.4610),
- fine-grained structural steel (DIN-No. 1.0566),
- cast steel (DIN-No. 1.1131, cast steel quality equivalent to fine grained structural steel),
- spheroidal cast iron (GGG 40.3, DIN-No. 0.7043),
- Ni-Resist D 2 (GGG-NiCr 20.2, DIN-No. 0.7660),
- Ni-Resist D 4 (GGG-NiSiCr 30.5.5, DIN-No. 0.7680),
- Si-cast iron (G-X 70 Si 15).

Ti 99.8-Pd, Hastelloy C4 and unalloyed steel are the reference materials in the joint European corrosive programme.

In 1983/1984 the two years experiments to influence of temperature (90°C, 170°C, 200°C) and gamma-radiation (10^5rad/h) on corrosion of the eight above mentioned materials were completed. The corrosive medium was a $MgCl_2$-rich quinary salt brine (Q-brine) representive for hypothetical accident conditions in a rock salt repository. Furthermore, the effect of different brines and material differences due to manufacturing process on the corrosion were investigated.

Besides the laboratory-scale experiments the in situ corrosion tests were continued in the Asse mine on material specimens at rock temperature ("reference experiment") and on electron beam welded tubes at 170°C. Moreover, the in situ tests were continued on the corrosion behaviour of Ti 99.8-Pd, Hastelloy C 4, cast steel and Ni-Resist D 4 exposed to high temperature, rock pressure and gamma radiation, which has been started within the frame work of the German/US Brine Migration Test.

2. Laboratory-scale corrosion studies

2.1 Experimental

2.1.1 Materials investigated

Table 1 shows the chemical composition of the investigated Ti 99.8-Pd, Hastelloy C 4, fine-grained structural steel, spheroidal cast iron, Si-cast iron, and the 2 Ni-Resists type D 2 and D 4. They will be denoted KfK-materials in this text. The materials Ti 99.8-Pd and Hastelloy C 4 were investigated as delivered (hot-rolled sheet metals, annealed, descaled) without any surface after-treatment. Due to the manufacturing process Ti 99.8-Pd exhibit a deformation layer of about 200 - 400 µm thickness which was covered by a non- uniform oxide layer (50 - 100 nm thickness). Prior to the corrosion tests the specimens of fine grained-structural steel (hot-rolled and annealed sheet metal), cast steel and spheroidal cast iron were freed by milling from the attached scale and casting skin, respectively. The material specimens of Ni-Resist D 2, Ni-Resist D 4 and Si-cast iron were investigated in the as delivered condition which means with the surface ground all-around.

Within the framework of the joint European corrosion programme additional comparative tests on material specimens of Ti 99.8-Pd, Hastelloy C4 and unalloyed steel were agreed by all participating countries to be carried out. These specimens being collected from the same melt and fabricated under identical conditions. These materials (EC-reference materials) are of the same type as the materials entered in Table 1 (KfK-materials), but they differ from the latter in their composition (Table 2) and in some cases in the structure and surface finish. In order to determine an influence possibly exerted by such manufacturing induced differences on the corrosion behaviour of the materials first comperative tests were performed on the EC-reference materials.

The essential differences of the EC-reference materials compared with the KfK-materials can be summarized as follows:

Ti 99.8-Pd

- composition: slightly lower content of Ti and Pd, approximately 3-fold O_2 content;
- structure: coarse-grained
- surface: smooth, as a result of chemical pickling. The surface of the corresponding KfK-material was mechanically descaled.

Hastelloy C 4

- composition: roughly 10-fold Fe content (0.56 wt.%), about 1 wt.% higher Ni content, and 0.2 - 0.3 wt.% lower Cr and Mo content;
- structure: hardly any difference detectable;
- surface: slightly rougher.

Low carbon steel

- composition: by a factor of 1.5 - 2 lower content of C, Si, Mn;
- structure: no line structure;
- surface: covered with a thick scale layer like the KfK material.

2.1.2 Testing conditions

The experimental conditions for the KfK materials (Table 1) and the EC-reference materials (Table 2) investigated have been summarized in Table 3. The materials were tested in brines which may be present under specified hypothetical accident conditions in a repository in rock salt. The composition at 55°C of the six brines used and their pH values have been entered in Table 4. In order to simulate additional up

take of pure NaCl in a HLW borehole at the higher disposal temperatures (200°C at the maximum), 1.7 g NaCl was added per 100 g of solution. The brines were selected on the basis of general knowledge available now of the occurence of potential brines in the Zechstein bodies of rock salt in Lower Saxony. The majority of the corrosion tests related to the quinary brine Q (26.8 wt.% $MgCl_2$, 4.7 wt.% KCl, 1.4 wt.% $MgSO_4$, 1.4 wt.% NaCl, 65.7 wt.% H_2) because this quinary brine is considered to be one of the most relevant solutions encountered in a accident case.

For all eight KfK-materials the influence of temperature and gamma-radiation on their corrosion behaviour in Q-brine was investigated. The three most promising materials, Ti 99.8-Pd, Hastelloy C 4 and fine-grained structural steel, were examined in addition in the other five brines indicated in Table 4. The testing temperatures in the absence of gamma irradiation were 90°C, 170°C and 200°C, the testing temperature under gamma irradiation was 90°C. The radiation source was a Co-60 source of about 3000 Ci. The radiation dose rate was 10^5 rad/h, corresponding to the dose rate on the surface of a thin-walled (thickness of about 5 mm) HLW-canister.

The temperature of 200°C corresponds to the maximum surface temperature of the HLW canisters according to the German borehole concept. The two additional temperatures were selected in order to investigate the influence of temperature on the material corrosion. The temperature of 170°C was chosen to have a comparison with the results of screening corrosion tests performed at this temperature. Finally the temperature of 90°C was selected because it is sufficiently below the boiling point (about 115°C) of Q-brine, allowing the tests to be carried out at normal pressure. The temperatures of 90°C and 170°C are also the reference temperatures at the joint European corrosion programme. The pressures of the corrosive media were normal pressure (at 90°C), 0.55 MPa, and 0.9 MPa (equillibrium pressures at 170°C and 200°C), respectively.

All corrosion tests were performed with a specimen surface to medium volume ratio of 1 $cm^2/5$ cm^3, i.e., for the case characterized by an excess in corrodant.

In order to test the corrosion resistance of the materials to weight changes, pitting corrosion, crevice corrosion, and stress corrosion cracking in the various corrosive media different specimen types had been manufactured. The weight changes due to corrosion were determined on plane specimens in the "as delivered" condition of the material. The sizes of specimens of Ti 99.8-Pd, Hastelloy C 4, fine-grained structural steel and EC-low carbon steel were 40 mm x 20 mm x 3-4 mm, for Si-cast iron 36 mm x 18 mm x 5 mm, and for the rest of cast materials 40 mm x 20 mm x 10 mm. Testing of Ti 99.8-Pd, Hastelloy C 4 and the steels for stress corrosion cracking was done with welded U-specimens (80 mm x 15 mm x 3-4 mm, limb spacing 18 mm) clamped with clamping joints made of the same material. On these specimens and on plane welded specimens also the influence of welding (TIG-welding) on corrosion was investigated. The bead always run in the center of the specimen vertically to its longitudinal direction.

To evaluate the susceptibility of the materials to pitting corrosion both the plane and the U-bent specimens were examined. The sensitivity of the materials to crevice corrosion was determined on two specimen types. In case of specimen type A a plane specimen of the test material (metal surface "as delivered") was contacted with a PTFE disc. In case of specimen type B two plane metal specimens were brought into contact and tightened by two PFTE nuts and bolts. In case of the latter specimen type both specimens with unworked surfaces ("as delivered") and specimens with polished surfaces (9 µm diamond paste) were investigated in order to determine the influence of the metal surface condition on corrosion.

All material specimens were cleaned in alcohol in an ultrasonic bath prior to immersion in the corrosive media. After removal from the corrosive media the specimens were freed from the adhering salt and corrosion products attached by a suitable pickling treatment in order to determine their weight changes.

The weight changes of the specimens were determined by gravimetry. The depth of any local corrosion attacks was determined by an electronic depth gauge and by taking surface profiles and metallographic micrographs. Three to four comperative specimens were used in all examinations.

The experimental set-ups have been described in an earlier publication /4/.

2.2 Results

2.2.1 Influence of temperature on the corrosion of base material and welded specimens in the quinary brine Q

2.2.1.1 General corrosion

The integral weight losses measured for the KfK materials (Table 1) in Q-brine after the maximum exposure time as well as the integral corrosion rates calculated from them have been entered in Table 5. The values are average values of 3-4 comperative specimens each.

General corrosion of Ti 99.8-Pd is characterized at all testing temperatures by a very low initial corrosion rate which decreases further with exposure time. Within the range investigated (90°C-200°C) the testing temperature had no noticeable influence on the corrosion rate of the material. After the maximum exposure period of 560 days the material corroded at all temperatures uniformly at a corrosion rate of only 0.17 µm/a.

The corrosion rate of Hastelloy C 4 increased with rising temperature but even at the maximum testing temperature of 200°C it remained low, namely about 0.2 µm/a. At 90°C (0.02 µm/a) and 170°C (0.17 µm/a) the corrosion rate remained constant over the entire period of testing. The values at 200°C, which are available now, suggest a decrease in corrosion rate with increasing exposure time.

The corrosion rates of the actively corroded /7/ fine-grained structural steel and cast steel had been, as expected, much higher than for Ti 99.8-Pd and Hastelloy C 4. Acid corrosion is considered to be the dominated process /8/ because at the temperatures investigated the pH-values of the Q-brine were all inferior to 4 (pH (25°C) = 4.8; pH (90°C) = 3.6). The influence of the O_2 on corrosion is negligible considering the long exposure periods involved here (>70 days) because the solubility of O_2 in the solution is low (<0.1 ppm at 90°C) and the limited amount of O_2 available in the closed testing systems is consumed after a short duration (about 3-7 days) for corrosive attack.

With increasing testing temperature the corrosion rates of the two unalloyed steels rose which is attributed to a thermally activated process and decreasing pH of the solution with rising temperature. In the lower temperature range between 90°C and 170°C the almost twofold increasing of temperature value caused an increase in the corrosion rate by a factor of about 3. The influence of temperature was maximum between 170°C and 200°C. In this case the corrosion rate of the steels increased by approximately the factor 6. At all temperatures the corrosion rates decreased with exposure period and, at the maximum exposure time attained so far of about 300-720 days, they were about 35 µm/a at 90°C, about 100 µm/a at 170°C, and 500-600 µm/a at 200°C.

Also for the cast materials, spheroidal cast iron, Si-cast iron, and the two Ni-Resists, the corrosion rates increased with increasing temperature, but even at 170°C it remained still low for the Ni-Resists (5 µm/a for type D 4, 15 µm/a for type D 2) and for Si-cast iron (11 µm/a). The corrosion rates of spheroidal cast iron (46 µm/a at 90°C, and 91 µm/a at 170°C, respectively) roughly corresponded to those of the steels.

2.2.1.2 Local corrosion, stress corrosion cracking

The results of the investigations relating to local corrosion (pitting, crevice, intergranular corrosion) after the maximum exposure time have been compiled in Tables 6 and 7.

After an exposure period of about three years Ti 99.8-Pd had still been free of attack by pitting corrosion and stress corrosion cracking. The optical micrograph in Figure 1 shows the uniform general corrosion of Ti 99.8-Pd by the example of a plane specimen immersed in Q-brine for 368 days at 170°C. The high resistance of Ti 99.8-Pd to local corrosion attacks is known to be due to the formation of a passive protective layer on the surface.

Surface examinations /9/ of corroded Ti 99.8-Pd specimens, "as delivered" and with polished surfaces, respectively, by means of electron spectroscopy (XPS, AES) revealed at all testing temperatures the presence of a passive layer consisting of TiO_2. The thickness of the layer (TiO_2 and Ti-suboxides) formed on the polished metal surface by oxidation in air increased after corrosion from about 2 nm to 4-6 nm. The TiO_2 layer of the "as delivered" specimens due to the manufacturing process varied between 50 nm and 100 nm. It was not possible to measure the change of thickness of this layer due to corrosion because it was within the variation of layer thickness of specimens prior to corrosion.

The studies related to crevice corrosion of Ti 99.8-Pd at 90°C and 170°C have revealed that the surface condition of the specimens has a significant influence on their behaviour to this type of corrosion. Specimens whose surfaces had been covered by a relatively thick TiO_2 layer (thickness 50-100 nm) due to the manufacturing process were resistant to crevice corrosion at the end of the maximum exposure period of about 580 days attained until now. On contrary, in specimens with polished surfaces and a thin TiO_2 layer of only about 2 nm formed in air, corrosion products were occured at the metal to metal contact area showing different interference colours (yellow, green-yellow, blue). However, at 90°C, no measurable attack by crevice corrosion had been detected, not even after 270 days. At 170°C corrosion attack took place at several points of the whole polished surface which attained a maximum depth of 50 µm after the maximum exposure period of roughly 270 days. This makes evident that a sufficiently thick TiO_2 layer must be present on Ti 99.8-Pd in order to avoid crevice corrosion.

After three years of exposure until now Hastelloy C 4 has remained resistant to pitting corrosion (micrograph, Fig. 2), and to stress corrosion cracking. However, it has been susceptible to crevice corrosion. At 90°C local crevice corrosion attacks occured at single points at the metal/PTFE and metal/metal contact surfaces with maximum depths of 250 µm (metal/PTFE), and 20-70 µm (metal/metal), respectively, after 500-600 days. At 170°C, practically the entire metal/metal contact surface was non-uniformly corroded and was covered with black corrosion products. In addition, the corrosion rate of the crevice specimens increased from 0.17 µm/a to 0.5 µm/a compared with that of the weight loss specimens. Nevertheless, crevice corrosion in the form of local corrosion attack was not measurable even after about 280 days at 170°C. It will be necessary to carry out tests of longer periods in order to establish whether the non-uniform general corrosion observed at 170°C is the start of local corrosion as in the case at 90°C.

Fine-grained structural steel and cast steel were resistant to pitting and crevice corrosion as well as stress corrosion cracking after an exposure period of up to two years. After short exposure periods in Q-brine they were attacked by corrosion with shallow pit formation and after extended exposure periods corrosion became a nearly uniform general corrosion. Figures 3 and 4 show characteristic micrographs of the steels after extended exposure periods in Q-brine at 170°C.

The two Ni-Resists, spheroidal cast iron and Si-cast iron, are attacked by pitting and intergranular corrosion after extended exposure periods. In case of the Ni-Resists an intermetallic phase consisting of Cr, Fe and Ni, which had been precipitated at the grain boundaries, was destroyed by corrosion whereas in case of spheroidal cast iron the iron was attacked which is a much less noble material than carbon. These effects caused deep holes in the specimens (see Table 6).

The TIG welded specimens of Ti 99.8-Pd, Hastelloy C 4, and fine-grained structural steel did not show significant differences in their corrosion behaviour compared with the parent material.

2.2.2 Influence of gamma-radiation on the corrosion in the quinary brine Q

The corrosion results of the materials tested in Q-brine at 90°C and 10^5 rad/h after the maximum exposure time have been compiled in Table 8. Figures 5 to 8 show as examples micrographs of Ti 99.8-Pd, Hastelloy C 4, and the two steels after long-time exposures.

All Ti 99.8-Pd specimens showed a slight weight gain. Its value after a exposure time of 609 days was 0.2 mg/cm².a. According to the results of investigations by /9/ the weight gain of the Ti 99.8-Pd specimens can be explained by the formation of a corrosion layer under the impact of irradiation which obviously forms faster than it decomposes. In these surface investigations has been shown that the oxide covering layer formed in the presence of radiation is thicker (600 nm after 609 days) by one order of magnitude than in the absence of radiation. Overlying the TiO_2 layer, which is typical for unirradiated specimens, a layer consisting of Mg and O was built up.

To estimate the general corrosion rate of the irradiated Ti 99.8-Pd specimens ist was assumed that the oxide covering layer consists only of TiO_2. The error caused by neglecting the MgO contribution should be small on account of the low thickness of the oxide layer and the minor differences in the density of TiO_2 ($4.1 g.cm^{-3}$) and MgO ($3.7 g.cm^{-3}$). On the basis of this calculation the general corrosion rate of Ti 99.8-Pd after 609 days is 0.7 µm/a and hence only slightly higher than in the absence of radiation. Furthermore Ti 99.8-Pd under irradiation was resistant to local corrosion (micrograph, Fig.5).

The specimens of all other materials investigated suffered from weight losses under irradiation which more much higher than in the absence of radiation. The corrosion rates calculated from these weight losses and entered in Table 8 increased under irradiation by about the factor 4 for spheroidal cast iron, by the factor 10-20 for the steels and Si-cast

steel, by the factor 40-60 for the two Ni-Resists, and by the factor 110 for Hastelloy C 4. These values should be considered as average values because the steels were subjected to non-uniform corrosion accompanied by shallow pit formation (micrographs in Figs. 7 and 8) whereas in the other materials strong pitting corrosion occured. However, judgeing from the surface diagrams and the metallographic investigations, the maximum depth of attack of shallow pit formation in the steels is only slightly higher than the average general corrosion rate. Moreover, it should be mentioned that the local corrosion attacks in Hastelloy C 4 (maximum pit depth 1 mm, maximum crevice corrosion depth 100 µm) had occured after long exposure periods (>130 days) which suggests a long period of incubation for pitting and crevice corrosion. The micrograph in Fig. 6 shows by way of example pitting corrosion for Hastelloy C 4.

The considerable increase in the corrosion rate of the materials exposed to gamma-irradiation, except for Ti 99.8-Pd, indicated that the strong oxidants formed during irradiation (e.g. H_2O_2, $^{\bullet}Cl_2^-$) act as cathodic depolarizers /6/.

The results of investigations under irradiation show that a gamma dose rate of 10^5 rad/h which has to be expected for a thin-walled HLW container (about 5 mm thick), exerts a strong influence on the corrosion behaviour of the materials investigated in Q-brine. By using thick-walled containers for mechanical resistance against the rock pressure (30-40 MPa) the surface dose rate and the resulting radiation effects are reduced significantly. Corrosion investigations at lower dose rates (10^2-10^4 rad/h) are in progress.

2.2.3 Influence of composition of different brines on the corrosion

In order to determine the influence of composition of the six brines in Table 4 on the corrosion behaviour of the most promising container materials, i.e. Ti 99.8-Pd, Hastelloy C 4 and fine-grained structural steel,

comparative experiments were performed at 170°C. The exposure period was six months. The testing results and the corrosivity of the testing media deduced from them have been summarized in Tables 9-11.

The results show that Ti 99.8-Pd and Hastelloy C 4 are highly resistant to corrosion in all testing media. Both materials corroded under the testing conditions with only a slight general corrosion and they were resistant to pitting corrosion. The thickness reduction of these materials in the various brines differs by only the factor 5 at the maximum. The different concentrations of the qualitatively equal brines Q and Z give differences in the thickness reduction of less than a factor 2 (Ti 99.8-Pd) and 1.2 (Hastelloy C 4), respectively. The maximum thickness reduction -although low in absolute terms- after six months of exposure occured for Ti 99.8-Pd in the Q-brine (0.16 µm) and in $CaCl_2$ (0.12 µm) and for Hastelloy C 4 in the Z-brine (0.37 µm) and Q-brine (0.33 µm).

The corrosion behaviour of fine-grained structural steel in the various testing media differed greatly both qualitatively and quantitatively (Table 11). The differences in the corrosivity of the testing media roughly amounted to a factor 36. In the KCl-, NaCl- and $CaCl_2$-brine the material corroded by slight general corosion (5.5-13 µm) and the corrosion attack was uniform (KCl-brine) or slightly non-uniform (maximum depth: 25-30 µm). General corrosion was likewise slight in the NaCl-$CaSO_4$ solution nevertheless in this medium shallow pit formation occured with a maximum depth of 200 µm. By contrast, in the Q- and Z-brine the fine-grained structural steel corroded almost uniformly with a high general corrosion. The differences in corrosivity of these two brines were only a factor of about 1.6 at the maximum.

The results of tests performed until now in the various brines confirm that the Q-brine, which had been used for the detailed corrosion studies, is one of the most aggresive corrosive media under postulated accident conditions in a repository in rock salt.

2.2.4 Influence of manufacturing induced material differences on corrosion

As already described in Section 2.1, the EC-reference materials Ti 99.8-Pd, Hastelloy C 4, and low carbon steel exhibit some manufacturing induced differences as compared to the equivalent KfK-materials. In order to examine whether these differences might influence corrosion, comparative investigations in Q-brine at 90°C and 170°C of up to one year duration will be performed on the EC-reference materials. The results obtained so far have been compiled in Table 12. For comparison, also the results applicable to the equivalent KfK-materials under comparable testing conditions have been entered in this table.

The corrosion rates, averaged over 180 to 300 days, of the EC-reference materials Ti 99.8-Pd (0.03 - 0.07 µm/a) and Hastelloy C 4 (0.17 to 0.57 µm/a) were low, corresponding so far to those of the KfK-materials. Also for the steels no noticeable differences in corrosion rate have so far been found after 75 to 90 days at 170°C (EC-steel: 256 µm/a, KfK-steel: 273 µm/a). At 90°C and about 70 days exposure until now the corrosion rate of the EC-steel of 122 µm/a was higher by about the factor 1.7 than that of KfK-steel.

On the basis of the results available no significant influence of the investigated manufacturing induced differences on corrosion is expected for Ti 99.8-Pd and Hastelloy C 4 at 90°C and 170°C.

Definite conclusions for the steels cannot be drawn from the results derived from the short-term experiments. For this purpose the results of the long-term studies must be awaited.

2.3 Conclusions

The following conclusions can be drawn from the results obtained so far on corrosion phenomena:

Among the materials studied, Ti 99.8-Pd exhibited the highest corrosion resistance. Under the selected testing conditions a reduction of the container wall thickness less than 1 µm/a can be anticipated, even in the presence of a gamma dose rate of 10^5 rad/h. The results obtained after a test period of up to 3 years, indicate no suceptibility to local corrosion or stress corrosion cracking. Nevertheless, further detailed investigations will be necessary to provide final evidence of the suitability of Ti 99.8-Pd as a material for long-term HLW containers. These will mainly involve clarification of questions relating to embrittlement in the presence of hydrogen and tensile stresses and to corrosion resistance to saline impurities (e.g. J^-, Br^-).

- Use of Hastelloy C4 as an HLW container material is restricted because of its susceptibility to pitting corrosion under gamma-irradiation and its sensitivity to crevice corrosion, both in the presence and in the absence of gamma-irradiation. HLW containers of this material can be used as an effective long-term barrier in a salt repository only if they are adequatly shielded against gamma-radiation and, if appropriate measures are taken to avoid narrow crevices. Studies are in progress to determine the treshold value below which the gamma dose rate must decline.

- For the unalloyed steels neither stress corrosion cracking nor local corrosion occured under the testing conditions so that their corrosion behaviour by general corrosion can be calculated. However, unalloyed steels must be sufficiently protected against gamma-radiation. In that case the corrosion rates for S/V = 1:5 cm^{-1} at 90°C (about 35 µm/a) and 170°C (about 100 µm/a) in a period of e.g. 300 years lead to corrosion allowances which are in the order of container wall thickness of about 10-30 mm. These values are relatively low in comparison to a estimated

wall thickness of 70 mm /10/ to ensure mechanical stability against the resulting rock pressure of 28 MPa. At 200°C, (corrosion rate: 500-600 µm/a) the necessary corrosion allowance will be greater than that for mechanical protection. Investigations are in progress to determine the wall thickness required to ensure that the gamma dose rate at the container surface and, consequently, the radiolysis of brines is reduced to negligible levels. In addition to these studies, further investigations will be necessary to qualify structural steels as HLW container material. This includes above all the determination of their susceptibility to H_2 embrittlement.

- The Ni-Resists, Si-cast iron and spheroidal cast iron must be ruled out as materials for long-term HLW containers because of their susceptibility to intergranuar and/or pitting corrosion.

On the basis of the corrosion results and under consideration of material costs, easy manufacturing and quality accurance concept we decided to use a unalloyed steel for the realization of a long-term HLW-container. To determine a reference steel comparative corrosion studies on different steels are in progress.

TABLE 1 CHEMICAL COMPOSITION OF KfK-MATERIALS USED IN TEST PROGRAMME

MATERIAL	COMPOSITION (wt.%)												
	Cr	Ni	Mo	Ti	Pd	C	Si	Mn	Nb	O_2	N_2	H_2	Fe
Ti 99.8-Pd (DIN No.3.7025.10)	-	-	-	BAL	0.17	0.01	-	-	-	0.04	0.01	0.001	0.05
HASTELLOY C 4 (DIN No. 2.4610)	16.8	BAL	15.9	0.33	-	0.006	0.05	0.09	-	-	-	-	0.05
FINE-GRAINED STEEL (DIN No. 1.0566)	-	-	-	-	-	0.17	0.44	1.49	-	-	-	-	BAL
CAST STEEL (DIN No. 1.1131)	-	-	-	-	-	0.16	0.61	1.51	-	-	-	-	BAL
SPHEROIDAL CAST IRON (DIN No. 0.7043)	-	-	-	-	-	3.7	1.83	0.21	-	-	-	-	BAL
Ni-RESIST D 2 (DIN No. 0.7660)	2.39	22.0	-	-	-	2.65	2.4	1.14	0.2	-	-	-	BAL
Ni-RESIST D 4 (DIN No. 0.7680)	5.5	30.9	-	-	-	2.6	4.25	0.5	-	-	-	-	BAL
Si-CAST IRON	-	-	-	-	-	0.72	15.0	0.62	-	-	-	-	BAL

- = NOT EXISTING OR NEGLIGIBLE

TABLE 2 CHEMICAL COMPOSITION OF EC-REFERENCE MATERIALS[1)]

MATERIAL	COMPOSITION (wt.%)												
	Cr	Ni	Mo	Ti	Pd	C	Si	Mn	Nb	O_2	N_2	H_2	Fe
Ti 99.8-Pd (DIN No.3.7035.10)	-	-	-	BAL	0.16	0.01	-	-	-	0.14	0.01	0.001	0.06
HASTELLOY C 4 (DIN No. 2.4610)	15.17	BAL	14.9	0.23	-	0.002	0.03	0.16	-	-	-	-	0.56
LOW CARBON STEEL	-	-	-	-	-	0.1	0.3	0.7	-	-	-	-	BAL

- = NOT EXISTING OR NEGLIGIBLE

1) EC-REFERENCE MATERIALS = MATERIALS USED FOR COMPARATIVE CORROSION TESTS IN THE JOINT EUROPEAN CORROSION PROGRAMME

TABLE 3 EXPERIMENTAL CONDITIONS FOR LABORATORY-SCALE CORROSION TESTS

	MATERIALS	CORROSION MEDIA[3]						TEMPERATURE/PRESSURE			GAMMA-IRRADIATION
		$NaCl - H_2O$	$KCl - H_2O$	$CaCl_2 - H_2O$	Q - BRINE	Z - BRINE	$NaCl-CaSO_4-H_2O$	90^oC/NORMAL PRESSURE	170^oC/0.55 MPa	200^oC/0.9 MPa	Q - BRINE $\dot{D} = 10^5$ rad/h $T = 90^o$ C NORMAL PRESSURE
KFK - MATERIALS[1]	Ti 99.8-Pd	X	X	X	X	X	X	X[4]	X	X[4]	X
	HASTELLOY C 4	X	X	X	X	X	X	X[4]	X	X[4]	X
	FINE-GRAINED STEEL	X	X	X	X	X	X	X[4]	X	X[4]	X
	CAST STEEL				X			X	X	X	X
	CAST IRON				X			X	X		X
	Ni-RESIST D 2				X			X	X		X
	Ni-RESIST D 4				X			X	X		X
	Si-CAST IRON				X			X	X		X
EC-REFERENCE MATERIALS[2]	Ti 99.8-Pd				X			X	X		
	HASTELLOY C 4				X			X	X		
	LOW CARBON STEEL				X			X	X		

X = INVESTIGATIONS PERFORMED; [1] COMPOSITION SEE TABLE 1;
[2] COMPOSITION SEE TABLE ; [3] COMPOSITION SEE TABLE 2; [4] ONLY IN Q-BRINE

TABLE 4 CHEMICAL COMPOSITION OF THE CORRODANTS AT 55° C

CORRODANT	COMPOSITION (wt.%)							pH (25° C)
	NaCl	KCl	$MgCl_2$	$MgSO_4$	$CaCl_2$	$CaSO_4$	H_2O	
NaCl - H_2O	26.9	-	-	-	-	-	73.1	7.2 ± 0.2
KCl - H_2O	-	30.7	-	-	-	-	69.3	6.4 ± 0.2
$CaCl_2$ - H_2O	-	-	-	-	57.4	-	42.6	2.9 ± 0.2 [1)]
NaCl-KCl-$MgCl_2$-$MgSO_4$-H_2O (Z - BRINE)	0.2	0.66	36.4	0.87	-	-	61.87	3.6 ± 0.2
NaCl-KCl-$MgCl_2$-$MgSO_4$-H_2O (Q - BRINE)	1.4	4.7	26.8	1.4	-	-	65.7	4.9 ± 0.2
NaCl-$CaSO_4$-H_2O	26.9	-	-	-	-	0.5	72.6	6.8 ± 0.2

1) AT 45° C

TABLE 5 GENERAL CORROSION OF INVESTIGATED MATERIALS IN Q-BRINE WITHOUT GAMMA-IRRADIATION AFTER THE MAXIMUM EXPOSURE TIME

MATERIAL	TEST TEMPERATURE (^{o}C)	MAXIMUM EXPOSURE TIME (d)	WEIGHT LOSS ($g \cdot m^{-2}$)	CORROSION RATE[1] ($\mu m \cdot a^{-1}$)
Ti 99.8-Pd	90	559	1.2 ± 0.07	0.17 ± 0.03
	170	529	0.46 ± 0.07	0.07 ± 0.03
	200	540	0.97 ± 0.07	0.14 ± 0.03
HASTELLOY C 4	90	559	0.26 ± 0.07	0.02 ± 0.02
	170	368	1.48 ± 0.07	0.17 ± 0.02
	200	540	2.69 ± 0.07	0.21 ± 0.02
FINE-GRAINED STEEL	90	285	213.3	35.0
	170	722	1505.0	97.4
	200	550	6946.0	590.0
CAST STEEL	90	586	421.3	33.4
	170	589	1169.6	92.2
	200	556	6077.3	507.6
SPHEROIDAL CAST IRON	90	465	405.2	45.8
	170	162	282.2	91.4
Ni-RESIST D 2	90	775	39.8	2.5
	170	589	179.9	15.1
Ni-RESIST D 4	90	775	34.4	2.1
	170	589	62.1	5.1
Si-CAST IRON	90	446	32.1	3.8
	170	448	92.0	10.8

1) CALCULATED FROM WEIGHT LOSS AND EXTRAPOLATED LINEARLY

TABLE 6 PITTING AND INTERGRANULAR CORROSION OF INVESTIGATED MATERIALS IN Q-BRINE WITHOUT GAMMA-IRRADIATION AFTER THE MAXIMUM EXPOSURE TIME

MATERIAL	TEST TEMPERATURE (°C)	MAXIMUM EXPOSURE TIME (d)	MAXIMUM PIT DEPTH (µm)	MAXIMUM INTERGRANULAR CORROSION DEPTH (µm)
Ti 99.8-Pd	90	559	-	-
	170	529	-	-
	200	540	-	-
HASTELLOY C 4	90	559	-	-
	170	368	-	-
	200	540	-	-
FINE-GRAINED STEEL	90	285	-	-
	170	722	-	-
	200	550	-	-
CAST STEEL	90	586	-[1)]	-[1)]
	170	589	-[1)]	-[1)]
	200	556	-[1)]	-[1)]
SPHEROIDAL CAST IRON	90	465	1300	-
	170	162	> 1300	-
Ni-RESIST D 2	90	775	-	450
	170	589	100	200
Ni-RESIST D 4	90	775	-	1600
	170	589	100	> 1600
Si- CAST IRON	90	446	300	500
	170	448	450	800

- = UNIFORM CORROSION

-[1)] = NON-UNIFORM CORROSION, NO PITTING OR INTERGRANULAR CORROSION

TABLE 7 CREVICE CORROSION OF INVESTIGATED MATERIALS IN Q-BRINE AFTER THE MAXIMUM EXPOSURE TIME

MATERIAL	SPECIMEN TYPE	SURFACE CONDITION	TEMPERATURE/ TIME	MAXIMUM CREVICE CORROSION DEPTH (µm)
Ti 99.8-Pd	A[1]	AS RECEIVED[3]	90°C/582 d	-
	B[2]	AS RECEIVED[3]	90°C/489 d	-
			170°C/286 d	-
		POLISHED (9 µm DIAMOND-PASTE)	90°C/266 d	-
			170°C/266 d	50+)
HASTELLOY C 4	A[1]	AS RECEIVED[4]	90°C/582 d	250++)
	B[2]	AS RECEIVED[4]	90°C/489 d	70+)
			170°C/286 d	-
		POLISHED (9 µm DIAMOND-PASTE)	90°C/266 d	20+)
			170°C/266 d	-
FINE-GRAINED STEEL	A[1]	DESCALED BY MILLING	90°C/421 d	-
	B[2]		90°C/124 d	-
			170°C/116 d	-

- = NON CREVICE CORROSION ATTACK

1) SIMULATED CREVICE BY CONTACTING METAL/PTFE

2) SIMULATED CREVICES BY CONTACTING METAL/METAL AND TIGHTENING WITH TWO PTFE NUTS AND BOLTS

3) SURFACE DESCALED MECHANICALLY, THICKNESS OF TiO_2-FILM 50-100 nm

4) SURFACE ETCHED IN H_2SO_4

+) AT THE INTERFACE METAL/METAL

++) AT THE INTERFACE METAL/PTFE

TABLE 8 GENERAL AND PITTING CORROSION OF INVESTIGATED MATERIALS IN Q-BRINE AT 90°C UNDER GAMMA-IRRADIATION (10^5 rad/h) AFTER THE MAXIMUM EXPOSURE TIME

MATERIALS	MAXIMUM EXPOSURE TIME (d)	WEIGHT CHANGE ($g \cdot m^{-2}$)	CORROSION RATE[2] ($\mu m \cdot a^{-1}$)	MAXIMUM PIT DEPTH (μm)
Ti 99.8-Pd	609	+ 3.53 ± 0.07	0.70 ± 0.02	-
HASTELLOY C 4	606	- 33.5 ± 0.07	2.3 ± 0.02	1000
FINE-GRAINED STEEL	244	- 2 425.0	464.2	-[1]
CAST STEEL	231	- 3 312.0	665.8	-[1]
SPHEROIDAL CAST IRON	173	- 545.0	165.2	220
Ni-RESIST D 2	160	- 507.9	157.4	160
Ni-RESIST D 4	160	- 257.0	77.1	200
Si-CAST IRON	153	- 163.7	55.8	250

- = UNIFORM CORROSION

-[1] = NON-UNIFORM CORROSION WITH SHALLOW PIT FORMATION

[2] CALCULATED FROM WEIGHT LOSS AND EXTRAPOLATED LINEARLY

TABLE 9 INFLUENCE OF BRINE COMPOSITION ON GENERAL CORROSION OF Ti 99.8-Pd AFTER 6 MONTHS IMMERSION AT 170° C (WITHOUT GAMMA-IRRADIATION)

CORRODANT	WEIGHT LOSS ($g \cdot m^{-2}$)	THICKNESS REDUCTION[1] (μm)	CORROSIVITY OF THE MEDIA (RELATIVE TO THE THICKNESS REDUCTION IN $NaCl - H_2O$)
$NaCl - H_2O$	0.13 ± 0.07	0.03 ± 0.02	1
$KCl - H_2O$	0.24 ± 0.07	0.05 ± 0.02	1.7
$NaCl-CaSO_4-H_2O$	0.31 ± 0.07	0.07 ± 0.02	2.3
$NaCl-KCl-MgCl_2-MgSO_4-H_2O$ (Z - BRINE)	0.35 ± 0.07	0.08 ± 0.02	2.7
$CaCl_2 - H_2O$	0.56 ± 0.07	0.12 ± 0.02	4
$NaCl-KCl-MgCl_2-MgSO_4-H_2O$ (Q - BRINE)	0.72 ± 0.07	0.16 ± 0.02	5.3

1) UNIFORM CORROSION; CALCULATION OF THICKNESS REDUCTION FROM WEIGHT LOSS

TABLE 10 INFLUENCE OF BRINE COMPOSITION ON GENERAL CORROSION OF HASTELLOY C 4 AFTER 6 MONTHS IMMERSION AT 170° C (WITHOUT GAMMA-IRRADIATION)

CORRODANT	WEIGHT LOSS ($g \cdot m^{-2}$)	THICKNESS REDUCTION[1] (μm)	CORROSIVITY OF THE MEDIA (RELATIVE TO THE THICKNESS REDUCTION IN $NaCl-CaSO_4-H_2O$)
$NaCl-CaSO_4-H_2O$	0.68 ± 0.07	0.08 ± 0.01	1
$KCl - H_2O$	0.70 ± 0.07	0.08 ± 0.01	1
$NaCl-H_2O$	0.70 ± 0.07	0.08 ± 0.01	1
$CaCl_2-H_2O$	0.99 ± 0.07	0.11 ± 0.01	1.4
$NaCl-KCl-MgCl_2-MgSO_4-H_2O$ (Q - BRINE)	2.9 ± 0.07	0.33 ± 0.01	4.1
$NaCl-KCl-MgCl_2-MgSO_4-H_2O$ (Z - BRINE)	3.2 ± 0.07	0.37 ± 0.01	4.6

1) UNIFORM CORROSION; CALCULATION OF THICKNESS REDUCTION FROM WEIGHT LOSS

TABLE 11 INFLUENCE OF BRINE COMPOSITION ON CORROSION BEHAVIOUR OF FINE-GRAINED STEEL AFTER 6 MONTHS IMMERSION AT 170° C (WITHOUT GAMMA-IRRADIATION)

CORRODANT	WEIGHT LOSS ($g \cdot m^{-2}$)	THICKNESS REDUCTION[1] (µm)	MAXIMUM PIT DEPTH (µm)	CORROSIVITY OF THE MEDIA (RELATIVE TO THE THICKNESS REDUCTION IN $KCl-H_2O$)
$KCl - H_2O$	43	5.5	-	1
$NaCl - H_2O$	59.4	7.6	25	4.5
$CaCl_2 - H_2O$	100.8	12.9	30	5.5
$NaCl-KCl-MgCl_2-MgSO_4-H_2O$ (Q - BRINE)	875.2	112	-	20.4
$NaCl-KCl-MgCl_2-MgSO_4-H_2O$ (Z - BRINE)	1000	128	-	23.3
$NaCl-CaSO_4-H_2O$	30.5	3.9	200	36.4

1) CALCULATED FROM WEIGHT LOSS

- = ALMOST UNIFORM CORROSION

Table 12 Comparison of the General Corrosion Results on EC-Reference Materials and KfK-Materials in Q-Brine

	Material	Test Temperature (°C)	Exposure Time (d)	Weight Losses ($g \cdot m^{-2}$)	Corrosion Rate [1] ($\mu m \cdot a^{-1}$)
EC-Reference Materials	Ti 99.8-Pd (DIN No.3.7035.10)	90	300	0.12	0.03
		170	245	0.213	0.07
	Hastelloy C 4 (DIN No. 2.4610)	90	180	0.75	0.17
		170	180	2.42	0.57
	Low Carbon Steel	90	69	180.6	122.4
		170	90	493.2	256.1
KfK - Materials	Ti 99.8-Pd (DIN No.3.7025.10)	90	310	0.92	0.24
		170	368	0.40	0.09
	Hastelloy C 4 (DIN No. 2.4610)	90	180	0.08	0.02
		170	180	0.72	0.17
	Fine-Grained Steel (DIN No. 1.0566)	90	75	111.0	69.0
		170	75	439.1	273.2

1) calculated from weight loss and extrapolated linearly to one year

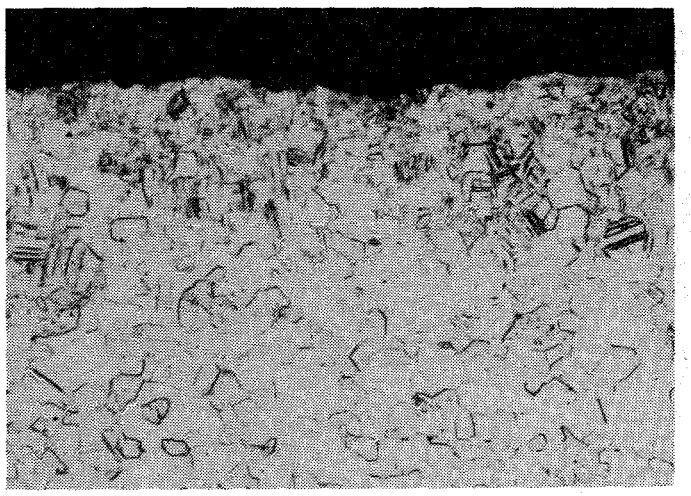

X 200, etched

FIG. 1 OPTICAL MICROGRAPH OF A SPECIMEN OF Ti 99.8-Pd IN AS-DELIVERED CONDITION AFTER 368 DAYS IMMERSION IN Q-BRINE AT 170° C WITHOUT GAMMA IRRADIATION

RESULT: UNIFORM CORROSION

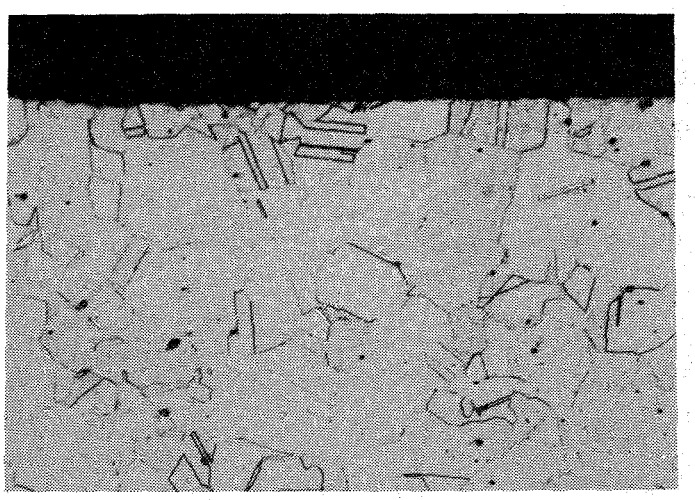

X 200, etched

FIG. 2 OPTICAL MICROGRAPH OF A SPECIMEN OF HASTELLOY C4 IN AS-DELIVERED CONDITION WITHOUT GAMMA IRRADIATION.
CORROSION CONDITIONS AS IN FIG. 1

RESULT: UNIFORM CORROSION

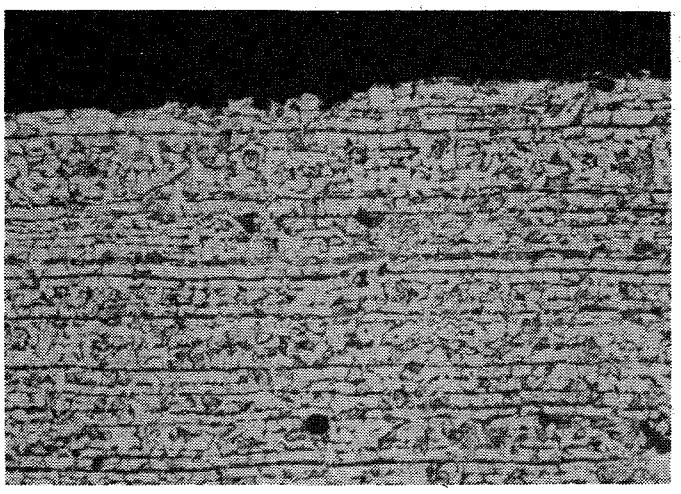

X 200, etched

FIG. 3 OPTICAL MICROGRAPH OF FINE-GRAINED STEEL SHOWING UNIFORM CORROSION AFTER 720 DAYS AT 170° C IN Q-BRINE

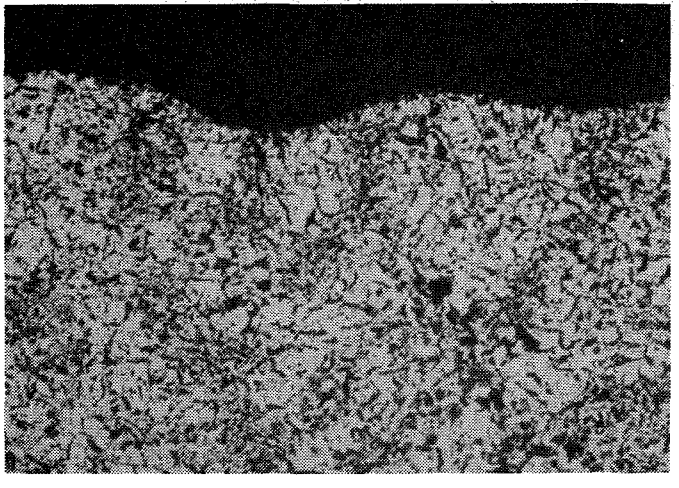

X 50, etched

FIG. 4 OPTICAL MICROGRAPH OF CAST STEEL SHOWING SLIGHTLY NON-UNIFORM CORROSION AFTER 590 DAYS AT 170° C IN Q-BRINE

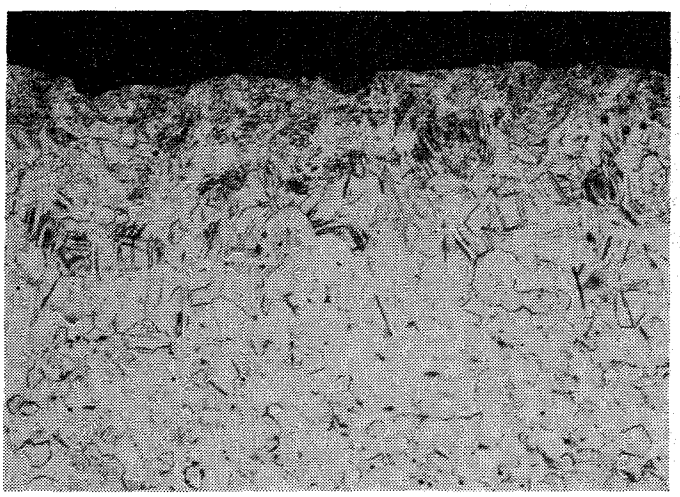

X 200 etched

FIG. 5 OPTICAL MICROGRAPH OF A SPECIMEN OF Ti 99.8-Pd IN AS-DELIVERED CONDITION AFTER 606 DAYS IMMERSION IN Q-BRINE AT 90° C WITH GAMMA IRRADIATION (10^5 rad/h)

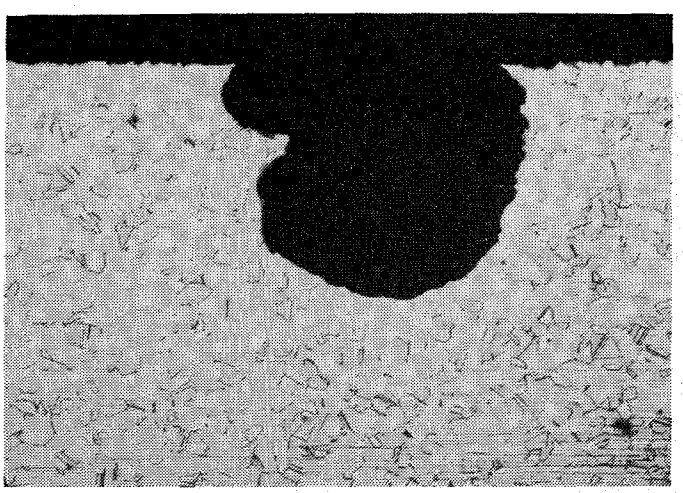

X 50 etched

FIG. 6 OPTICAL MICROGRAPH OF A SPECIMEN OF HASTELLOY C4 IN AS-DELIVERED CONDITION WITH GAMMA IRRADIATION (10^5rad/h). CORROSION CONDITIONS AS IN FIG. 3.

RESULT: PITTING CORROSION

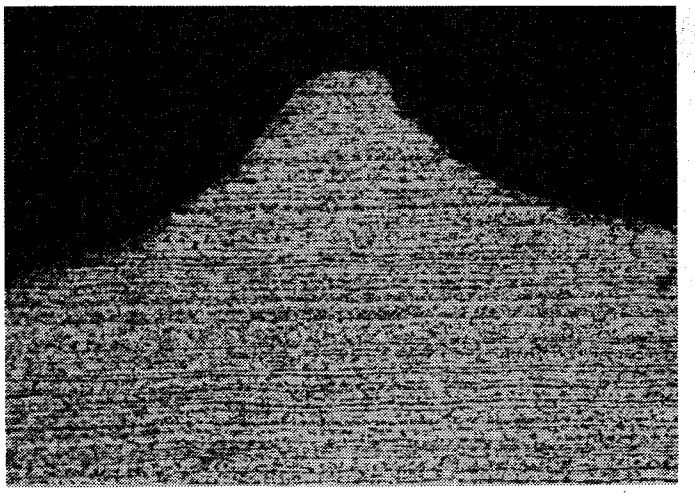

X 100, etched

FIG. 7 OPTICAL MICROGRAPH OF FINE-GRAINED STEEL SHOWING SHALLOW PIT CORROSION AFTER 245 DAYS AT 90° C AND 10^5 rad/h GAMMA IRRADIATION IN Q-BRINE

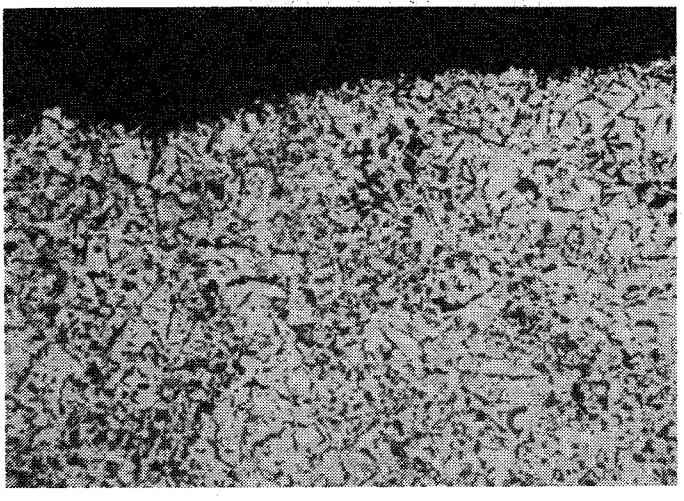

X 50, etched

FIG. 8 OPTICAL MICROGRAPH OF CAST STEEL SHOWING SHALLOW PIT CORROSION AFTER 230 DAYS AT 90° C AND 10^5 rad/h GAMMA IRRADIATION IN Q-BRINE

3. In situ corrosion experiments (field tests)

In the in situ experiments conducted in the Asse salt mine the corrosion behaviour of base material as well as of welded specimens and tubes is investigated under the conditions prevailing in the rock salt. Detailed information about the anticipated composition of the corrosive medium (NaCl with low contents of $CaSO_4$ and $K_2MgCa_2(SO_4)_4 \cdot 2\,H_2O$) and about brine migration in the temperature gradient can be found in /11, 12/. Figure 9 shows the site and location of the test field.

Within the frame of the in situ corrosion tests the following investigations are being performed on the materials titanium- palladium (Ti 99.8-Pd), Hastelloy C 4, cast steel (GS 16 Mn 5), and Ni-Resist, type D4:

- Investigation of base material and welded specimens (sheets) in loose rock salt (salt drilling dust) at rock temperature of about 35°C (reference experiment). The testing period is 1-3 years.

- Investigation of specimens in the German/US Brine Migration Test Field in 5 m deep boreholes at 210°C, an anticipated rock pressure of about 30 MN/m^2, and a gamma dose rate (Co-60 source) of $3.4.10^4$rad/h. In this experiments brine migration as well as the formation of gas due to corrosion and radiolysis are being measured continuously.

- Examination of tubes with a simulated container closing technique by electron beam welding in 2 m deep boreholes drilled into rock salt at 170°C and at the rock pressure resulting from convergence.
The testing period is 1-3 years.

During the period 1980-82 a detailed in situ test concept was elaborated /4/ and preparation of material specimens, procurement of testing equipment, and setting up of the in situ preliminary tests were determined.

In 1983-84 period the following work was performed for the in situ experiments:

- manufacturing of the welded tubes,
- evaluation of the in situ preliminary tests,
- preparation of the test field,
- installation of measuring equipment in the test field,
- installation of the welded tubes and starting operation of the test field.
- storage of material specimens of Ti 99.8-Pd, Hastelloy C 4, cast steel (GS16Mn5), and Ni-Resist, type D 4 in loose salt at rock temperature as well as in the Brine Migration Test Field at 210°C, under gamma-radiation, and at an anticipated rock pressure of 30 MN/m^2.

3.1 Experiments on base material and welded specimens

For reference investigations at rock temperature material specimens of Ti 99.8-Pd, Hastelloy C 4, cast steel, and Ni-resist D 4 were stored in 200 mm deep boreholes (36 mm in diameter) and covered with the salt drilling dust. The testing temperature is 35°C, the maximum testing period scheduled is 4-5 years. The chemical composition of the materials are shown in Table 1. The first specimens were recovered after six month storing. As expected, neither changes in weight nor local corrosion phenomena have been detected on the specimens.

Besides the investigations above, material specimens consisting of the materials indicated before were stored for in situ investigation of their corrosion behaviour under the impact of high temperature, rock pressure and gamma-radiation (Co-60 source) within the frame of the Brine Migration Test.

The conditions are:

- site : Asse salt mine (800 m floor)
- test set-up : see Fig. 24
- pressure loading: 28 MN/m^3 at the maximum
- temperature : 210°C at the maximum
- storage period : about three years
- gamma dose rate : 3.4×10^4 rad/h

During the test the rock pressure and the temperature at the borehole wall are being measured on-line and the climate in the borehole is being recorded. The test was started mid-1983, the specimens are scheduled for recovery in late 1986.

3.2 Experiments on welded tubes

In the in situ corrosion tests on welded tubes the corrosion behaviour of the materials is tested under the influence of simulated manufacturing and repository conditions.

They include:

- welding and heat treatment,
- geometry and surface finishing,
- stresses applied in the manufacturing process
- axial and radial temperature gradients in the circular gap between the tubes and the borehole wall,
- heat transfer and potential differences on the tube surface
- rock pressure due to convergence.

Moreover, by examinations of welded tubes knowledge is to be provided for the optimum design and execution of subsequent cost-intensive integral experiments (product and packaging) on the full scale.

3.2.1 Manufacturing of tubes

In accordance with the selected HLW packaging concept /13/ consisting in thick-walled steel containers with or without corrosion protection, four types of tubes were manufactured of each material. They were:

type I : tubes of cast steel GS 16 Mn 5,
type II : tubes of Ni-Resist D 4,
type III : basic body made of cast steel plated with Ti 99.8-Pd,
type IV : basic body similar to type III, but plated with Hastelloy C 4.

Figure 10 shows the layout of the tubes. The chemical compositions of the materials used are evident from Table 13.

In order to simulate the container closing technique electron beam welding was selected as the joining technique. It offers the following advantages in the practical case under consideration (design in conformity with protection against corrosion):

- little heat affected zone and hence little influence on the structure of the material,

- avoiding impurities of the structure by gas accommodation (welding in the vacuum chamber),

- little change of shape and hence low shrinkage,

- welding without filler metal,

- high degree of automation and good reproducibility of the optimum welding parameters determined and, consequently, possibility of quality assurance by process control.

The optimum parameters (Table 14) for welding the tubes were determined by test weldings*) on material specimens. Using the optimum welding parameters, also corrosion specimens for laboratory testing were welded in addition to the tubes. The appearance of these joints on corrosion specimens of the materials cast steel, Ni-Resist D 4, Hastelloy C 4, and Ti 99.8-Pd is shown by the micrographs in Figs. 11 to 14.

Manufacture of laboratory-scale corrosion specimens by electron beam welding (EB) serves the following purposes:

- comparison with material specimens prepared by tungsten inert gas welding (TIG) as regards the quality of the welding seam;

- determination of the influence exerted by the welding techniques applied (EB, TIG) on the corrosion behaviour of the materials;

- comparison of corrosion phenomena found in laboratory specimens with corrosion phenomena found on the tubes stored in situ.

The sequence of tubes manufacturing can be seen in Table 15 and Fig. 15. The SEM-pictures of selected points on the surface of a tube explosion plated with Ti 99.8-Pd is shown in Fig. 16 by way of example.

*) performed at the Institut für Kerntechnik und Energieumwandlung der Universität Stuttgart

3.2.2 Evaluation of the in situ preliminary tests

After a duration of the in situ preliminary tests (three boreholes for storage) of 298 days (set-up, see Fig. 17) the following statements can be made:

- Trouble-free operation of the heater types installed (heater cartridges of d = 20 mm and l = 300 mm) under the prevailing operating conditions and independent of the heat power (500, 1000, 1500 W) suggests that an adequate service life of the heater cartridges can be expected.

- Constant temperatures in the zone of contact between the tubes and the wall of the storage borehole established after two hours of heating at the maximum. The temperature which can be adjusted by controls in the zone of contact mentioned before was kept constant within $\pm$ 1°C during the entire period of preliminary testing.

- The measured temperatures at the sealing (see Fig. 17) had constant value of 55°C and hence lay well below the maximum admissible temperature of the O-rings of 100°C in permanent operation.

- The temperature loading of the heater supply line will be 100°C at the maximum and hence be well below the maximum admissible service temperature of 25°C of the insulating sheath.

- The voltage of the main supply of the Asse mine during the period of preliminary testing were

  - maximum voltage: 255 V
  - minimum voltage: 200 V
  - maximum variations in voltage: 40 V, temporarily
  - mean variations in voltage : 15 V.

The voltage above did not impair test operation. 16 power failures in total with an aggregate outage time of about 16 days were recorded. The resulting temperature drop in the zone of contact between the tube and the wall of the borehole was 50°C at the maximum. However, in 80% of all failures the temperature drop was $<$20°C.

According to /14/ this type of temperature drops may lead to cracking in the surrounding rock salt and hence an increased release of brine. Consequently, the conditions in the in situ corrosion tests will probably be more stringent than in the future practical case of HLW waste form disposal (continuous heat release).

- Retrieval of the three stored tubes of carbon steel by overcoring (Fig. 18) did not cause any problems. Overcoring ensures the safe retrieval of the tubes with a zone of 300 mm length (heated zone) to be subjected to post-examination. Borehole shrinkage within the heated zone was 1 mm in diameter.

During the testing period of 1 year no corrosion phenomena were observed on the tubes of carbon steel in rock salt.

3.2.3 Preparation of the test field

For storing of the tubes and for monitoring by instruments 20 boreholes in total*) were drilled with a profile corresponding to that in Fig. 19. The spacing of the boreholes was 2 m each.

Inspection of the borehole wall with an endoscope did not reveal irregularities such as effluorescence in the rock salt. The surface of the borehole wall has been represented in Fig. 19 as representative of all boreholes drilled for storage.

---

*) performed by the service department of the Asse salt mine

The representative salt drilling dust was characterized by a detailed chemical analysis which included the assay of the water content**). The results in Table 16 show that the rock salt is very pure and dry.

In order to simulate a possible brine migration towards the tubes, 100-200 ml brine each were metered into the gap between the tubes and walls of 12 of the 16 boreholes drilled for storage. The following brines were used:

- saturated NaCl solution without and with impurities (e.g. I^-, Br^-),
- saturated MgCl-rich quinary brine (Q-brine).

3.2.4 Measuring equipment of the test field

In the course of development of the testing concept and based on findings of the preliminary test evaluation the test programme was extended to the following items:

- measurement of water content of rock salt as function of distance from the exposure borehole. Earlier in situ experiments /15/ suggest that water/brine inclusions in the rock salt are likely to migrate towards the heat source from the vicinity of the storage boreholes at the testing temperature of 170°C. A temperature drop in the boreholes as a result of main supply failure could give rise to cracking in the near field of the boreholes and hence to augmented release of water. To enable interpretation of the results of corrosion tests on the

*) performed at the Institut für Tieflagerung (Braunschweig) der Gesellschaft für Strahlen- und Umweltforschung

tubes temporal changes in equilibrium humidity at a radial distance from the heated zone will be determined using a capacitive humidity detector /16/. Additional data for water content in the near field of the storage boreholes will be obtained by the chemical analysis of drilling samples taken in the radial direction of the stored tubes. The drilling kernels are extracted as shown in Fig. 20.

- measurements of the change of initial gap width (1 mm) between the tubes and the borehole wall due to thermally induced convergence as well as determination of the developing rock pressure using strain gauges applied to the outer diameter of the tubes. This should provide better understanding of the corrosion conditions prevailing during the test.

  Thermocouples have been installed, as shown in Fig. 21, for the purpose of monitoring axial temperature distribution on the tube wall and of determining the radial temperature distribution in the rock salt. To evaluate the pressure load acting on the tubes resulating from thermally induced convergence of the rock salt two tubes have been installed with strain gauges applied to their external walls (Fig. 21). In order to record the temporal changes in equilibrium humidity a humidity detector /16/ has been installed; see Fig. 21.

3.2 Start of operation

The tubes (16 in total) were installed as shown in Fig. 22. In order to simulate a tight closure of the borehole the upper part of the circular gap was tightly sealed with a cast resin. By a functional control of the power supply, heater function and the measuring and control equipment the readiness for operation of the test field (Fig. 23) was guaranteed. After drafting an operation plan by the Bergamt Goslar (mining authority) and after its approval in confirmity with mining regulations operation started in March 1985. An Overview of the test field is given in Fig. 23.

MATERIAL	FE	C	SI	MN	MG	CO	CR	MO	NI	NB	TI	PD	S	P	N_2	O_2	H
	WEIGHT %																
HASTELLOY C4 No. 2.4610[1)]	0.84	<0.002	0.02	0.17	-	<0.1	15.54	15.28	BASIS	-	0.24	-	<0.002	<0.005			
TI 99.8-Pd No. 3.7025.10[2)]	0.03	<0.05	-	-	-	-	-	-	-	-	BASIS	0.18	-	-	0.015	0.16	<0.006
CAST STEEL GS 16 Mn5[3)]	BASIS	0.16	0.66	1.51	-	-	-	-	-	-	-	-	0.011	0.013			
Ni-RESIST D4 No. 0.7680[4)]	BASIS	1.89	5.4	0.5	0.081	-	5.05	-	30.0	0.21	-	-	0.005	0.028			

- = NOT PRESENT OR NEGLIBLE

1) CABOT CORPORATION, 1020 WEST PARK AVENUE, KOKOMO, INDIANA 46901, TEST No. 81 081 1136

2) TITANIUM INTERNATIONAL, DÜSSELDORF, TEST No. L 848

3) STAHLWERKE PEINE, SALZGITTER, FACTORY CERTIFICATE No. 66/83/G

4) BUDERUS, FACTORY CERTIFICATE No. 82/786

TABLE 13: CHEMICAL COMPOSITION OF THE WELDED TUBE MATERIALS USED IN THE IN SITU-CORROSION TESTS

WELDING PARAMETERS / MATERIAL	SPECIMEN SIZE mm / SPECIMEN TREATMENT	BEAM CURRENT INTENSITY m A	ACCELERATOR VOLTAGE kV	WORKING DISTANCE mm	WELDING VELOCITY mm/s	SHAPE OF DEFLECTION AND FREQUENCY Hz	TRANSVERSE CONTRACTION mm
CAST STEEL GS - 16 MN 5	10x20x40 - groove faces milled - degreased	top bead 17.5 bottom bead 3.0	140	150	10	double parabola 310	0.05 - 0.1
NICKEL RESIST D4 No. 0.7680	10x20x40 - groove faces milled - degreased	top bead 12.0 bottom bead 5.0	140	145	10	double parabola 310	
TITANIUM - PALLADIUM No. 3.7025.10	3x20x40 - groove faces milled - decreased - pickled	top bead 9.0 bottom bead 3.0	140	150	30	circular weaving 570	0.1
HASTELLOY C4 No. 2.4610	4x20x40 - groove faces milled - decreased - pickled	top bead 11.0 bottom bead 4.0	140	150	20	circular weaving 760	$\leq$ 0.05

TABLE 14: OPTIMIZED WELDING PARAMETERS (IN SITU-CORROSION EXPERIMENT)

SEQUENCE OF MANUFACTURING OPERATIONS	BASE MATERIAL DELIVERY CONDITION	CORROSION PROTECTION MATERIAL DELIVERY CONDITION	FINISHING BASE MATERIAL	FINISHING CORROSION PROTECTION MATERIAL	FINISHING OF BASE MATERIAL AND CORROSION PROTECTION MATERIAL	SIMULATED CLOSING TECHNIQUE	DOCUMENTATION AND TESTING PROGRAMME
No. I (Fig. 11)	GS - 16 Mn 5 round rods Ø 50, 500 mm long, annealed	similar to base material	unilateral cutting by turning and boring surface quality		———	- joining pipe segments by electric beam welding - low tension annealing (2 h, 700°C)	- visual inspection of surface - surface profiles dimension protocol - micrograph of initial material and of one model seam each - crack inspection by ultrasound - SEM pictures of selected points
No.II (Fig. 11)	GGG-NiSiCr 30.5.5 Nb round rods Ø 50, 500 mm long annealed	similar to base material			———	- joining pipe segments by electron beam welding with Hastelloy C4 interlining	
No.III (Fig. 11)	similar to No. I	Ti 99.8 Pd pipes with longitudinally welded seams, inert gas welded by machines, seams untreated, pressurized and pickled	similar to No.I	turning out pipe internal dia. and cutting to length as a preparation for explosive plating	- explosive plating of the corrosion protection material onto the base material - overturning of pipe external diameter	joining pipe segments by providing cover strips and by electric beam welding	
No.IV (Fig. 11)	similar to No. I	Hastelloy C4 pipes with longitudinally welded seams, inert gas welded by machines, seams untreated, pressurized and pickled	similar to No. I	"	"	"	

TABLE 15: SEQUENCE OF WELDED TUBES (IN SITU-CORROSION EXPERIMENT)

BOREHOLE FOR STORAGE No. / COMPOSITION OF SALT DRILLING DUST		MEASURING FIELD				WELDED TUBES MADE OF Ni-RESIST				WELDED TUBES MADE OF GS-16 Mn 5				WELDED TUBES MADE OF Ti 99.8 Pd				WELDED TUBES MADE OF HASTELLOY C4			
		1	2	3	4	5	6	7	8	9	10	11	12	13	14	15	16	17	18	19	20
Na^+	wt.%	36.07	37.81	37.06	28.32	38.94	38.93	38.71	38.34	37.94	37.75	36.91	37.49	36.8	37.74	37.84	37.96	37.8	35.29	36.09	37.27
K^+	"	0.6	0.18	0.24	0.11	0.07	0.05	0.19	0.33	0.1	0.1	0.18	0.23	0.21	0.35	0.28	0.23	0.34	0.59	0.45	0.39
Li^+	"	-	-	-	-	-	-	-	-	-	-	-	-	-	-	-	-	-	-	-	-
Ca^{++}	"	1.71	0.82	1.18	0.48	0.15	0.14	0.22	0.17	0.93	1.07	1.63	1.16	1.68	0.84	0.89	0.8	0.8	2.4	1.97	1.14
Mg^{++}	"	0.17	0.07	0.07	0.07	0.06	0.1	0.05	0.16	0.03	0.04	0.06	0.06	0.07	0.1	0.08	0.07	0.09	0.19	0.13	0.1
Cl^-	"	54.73	57.34	54.71	58.06	59.88	60.23	59.12	58.02	58.51	58.25	57.05	58.03	56.93	58.41	59.07	58.76	58.4	54.7	55.88	57.53
SO_4^{--}	"	6.71	3.78	6.73	2.96	0.9	0.54	1.72	2.97	2.48	2.79	4.17	3.03	4.31	2.55	1.83	2.18	2.56	6.84	5.48	3.56
WATER mg/kg	"	2.39	0.59	0.49	0.76	0.15	0.17	0.48	1.05	0.66	0.52	0.95	1.83	1.37	2.26	1.59	1.3	1.99	3.65	2.92	2.23

data from GSF, Institut für Tieflagerung (Braunschweig)

TABLE 16: ANALYTICAL DATA ON ROCK SALT DRILLING DUST (IN SITU-CORROSION EXPERIMENT)

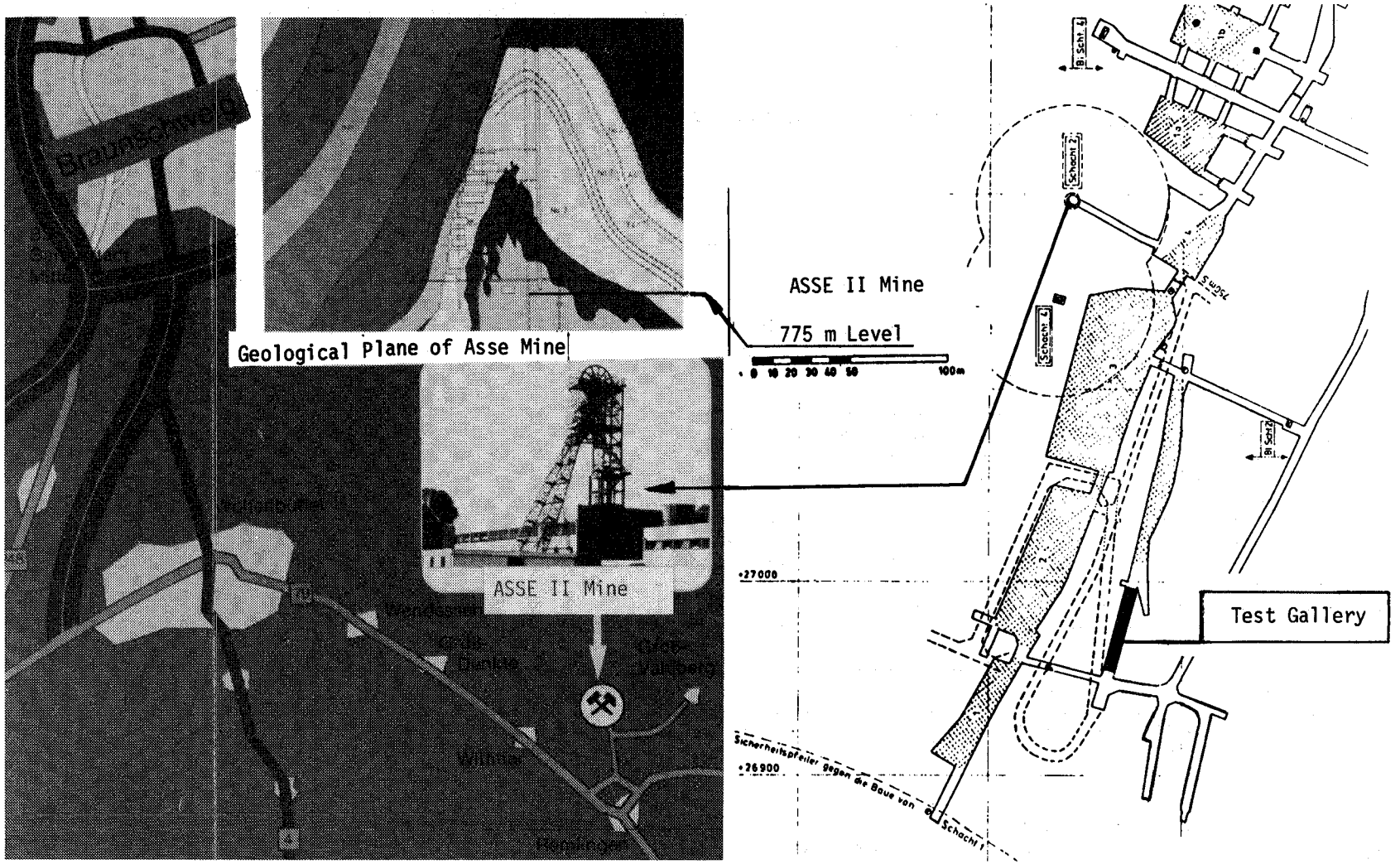

FIG. 9 SITE AND LOCATION OF THE IN SITU-TEST FIELD

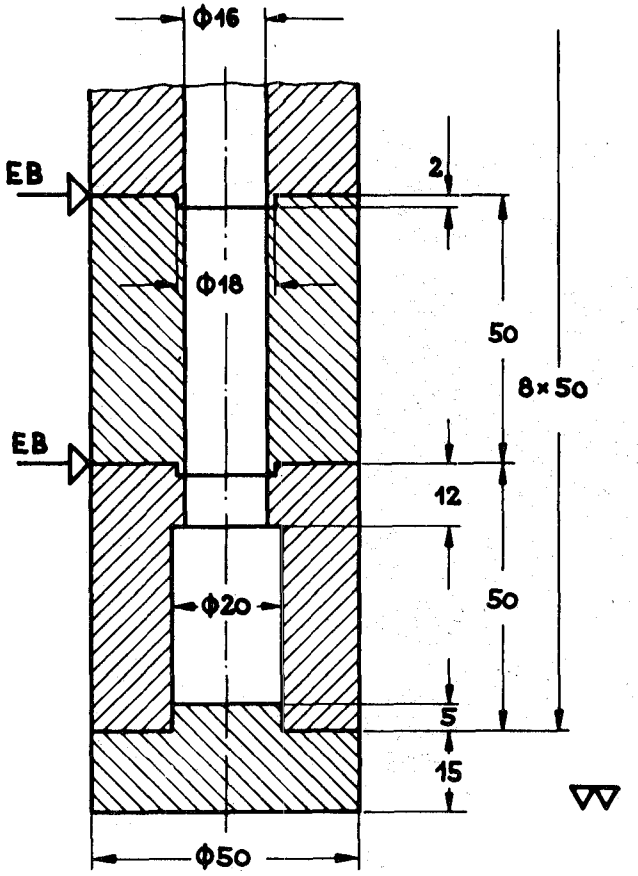

Canister type I: cast steel GS-16 Mn5

II: GGG-NiSiCr-30.5.5 Nb

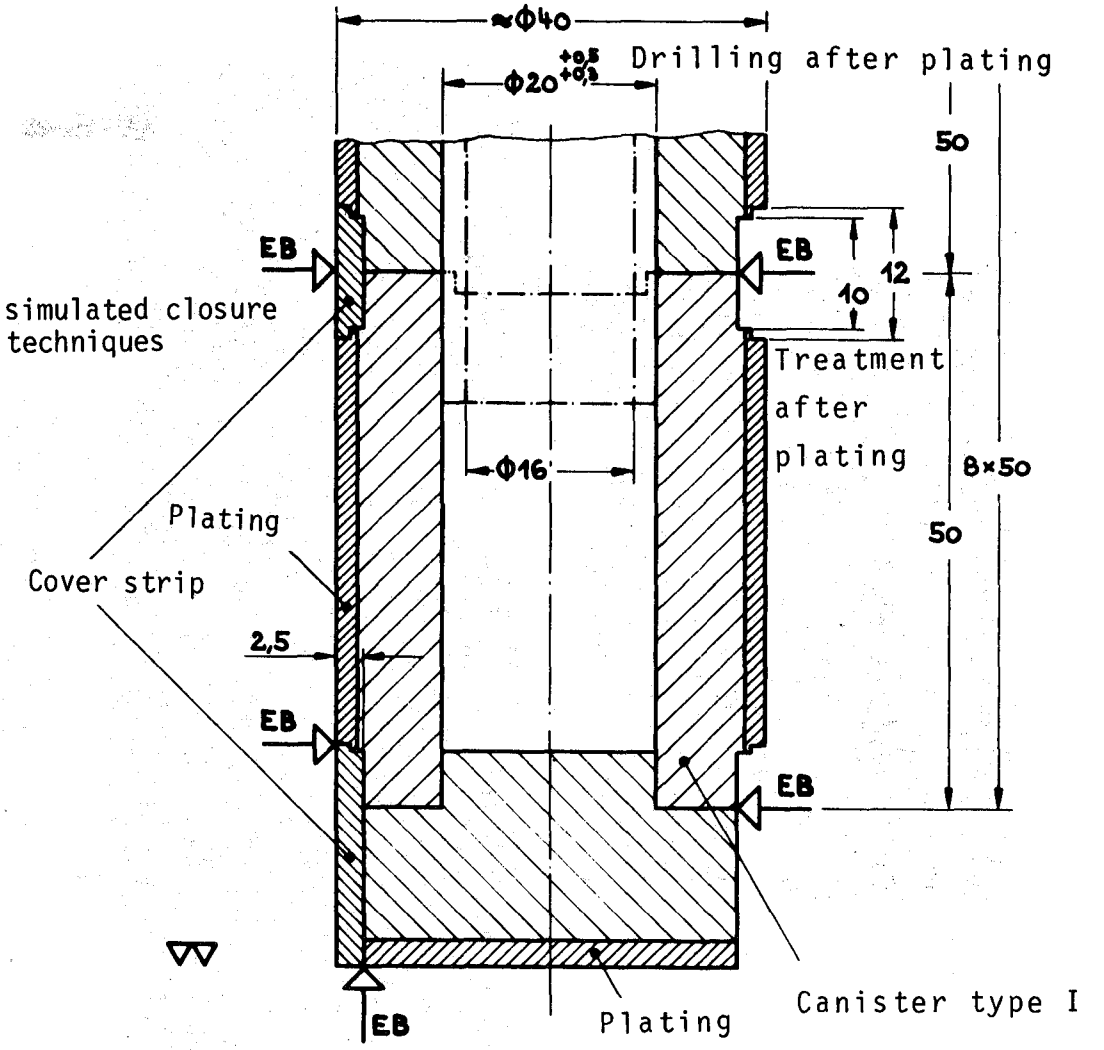

Canister type III: Ti99.8-Pd plated

IV: Hastelloy plated

FIG. 10: ASSEMBLY OF MODEL CONTAINERS (IN SITU-CORROSION TEST)

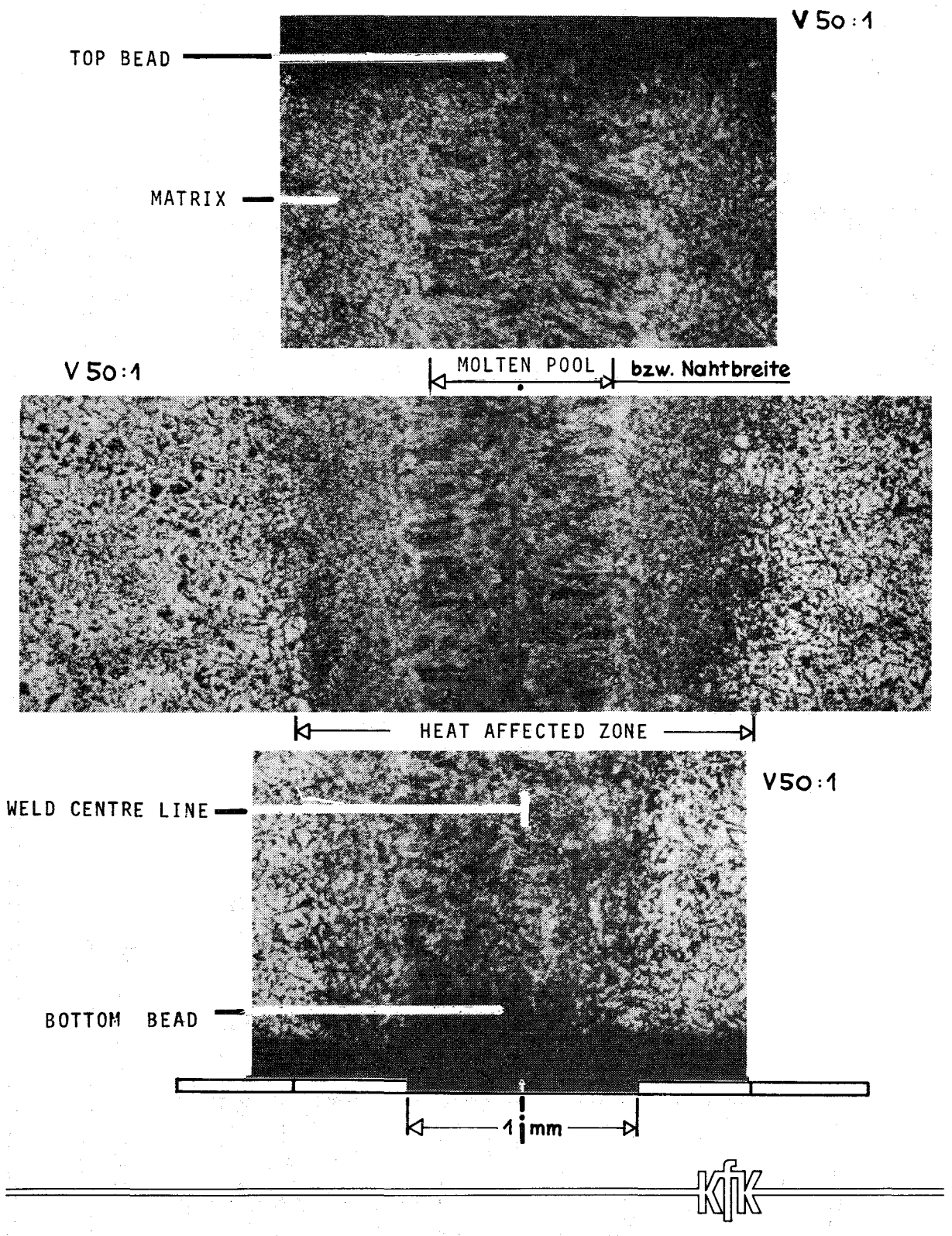

FIG. 11: TRANSVERSE MICROGRAPH OF AN ELECTRON BEAM WELDED CAST STEEL SPECIMEN (IN SITU-CORROSION TEST)

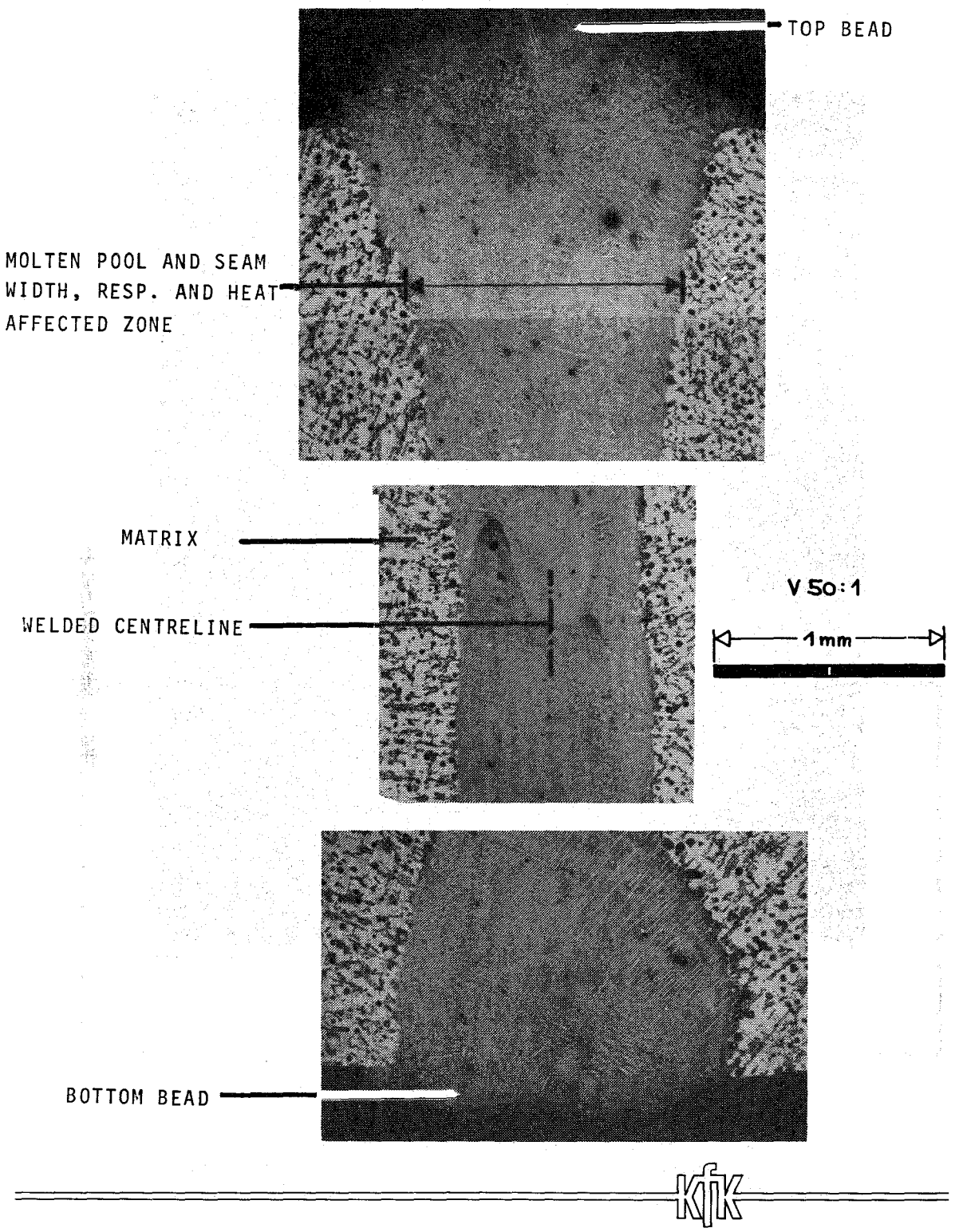

FIG. 12: TRANSVERSE MICROGRAPH OF AN ELECTRON BEAM WELDED Ni-RESIST D4 SPECIMEN (IN SITU-CORROSION TEST)

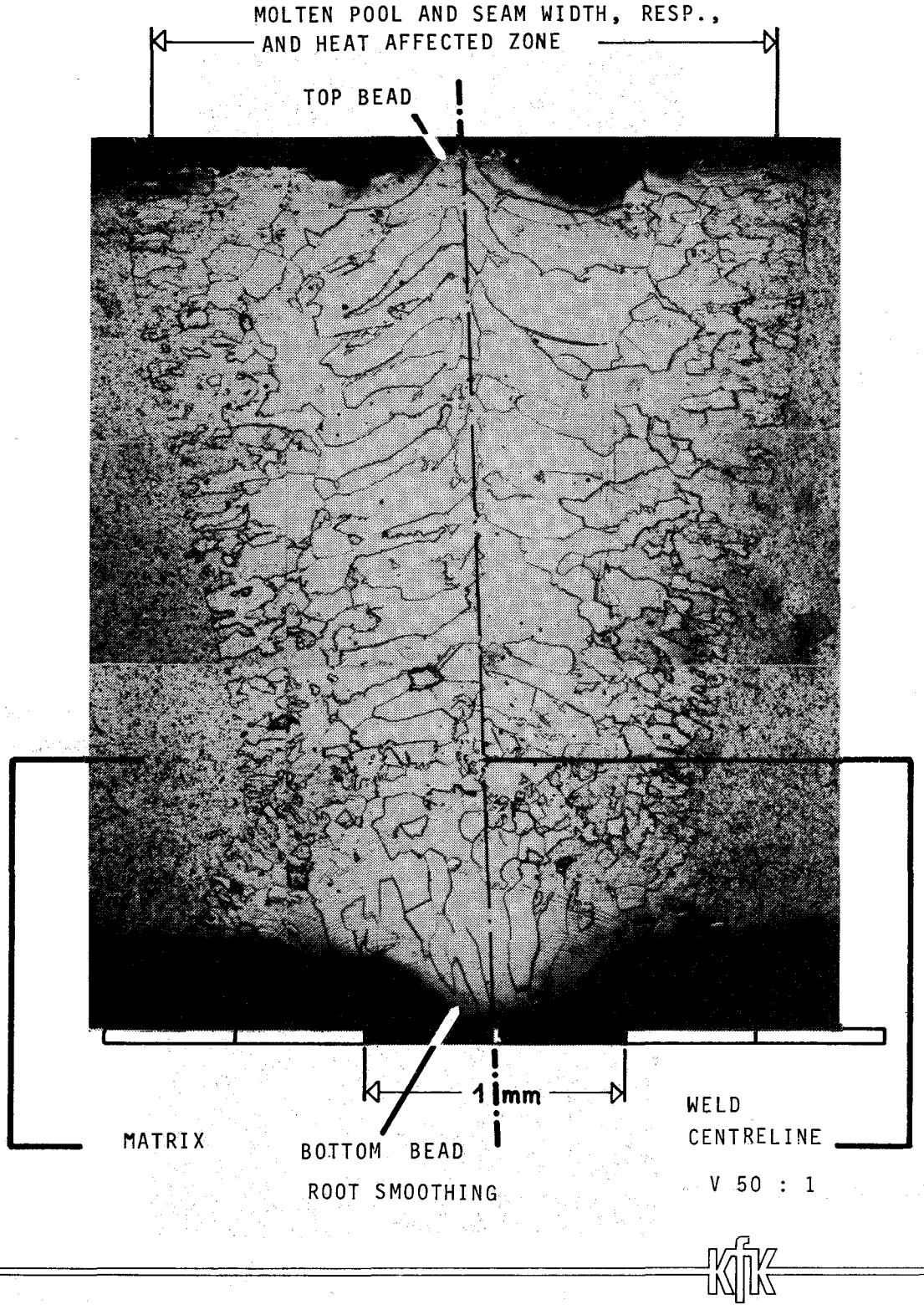

FIG. 13 TRANSVERSE MICROGRAPH OF AN ELECTRON BEAM WELDED Ti-99.8 Pd SPECIMEN (IN SITU-CORROSION TEST)

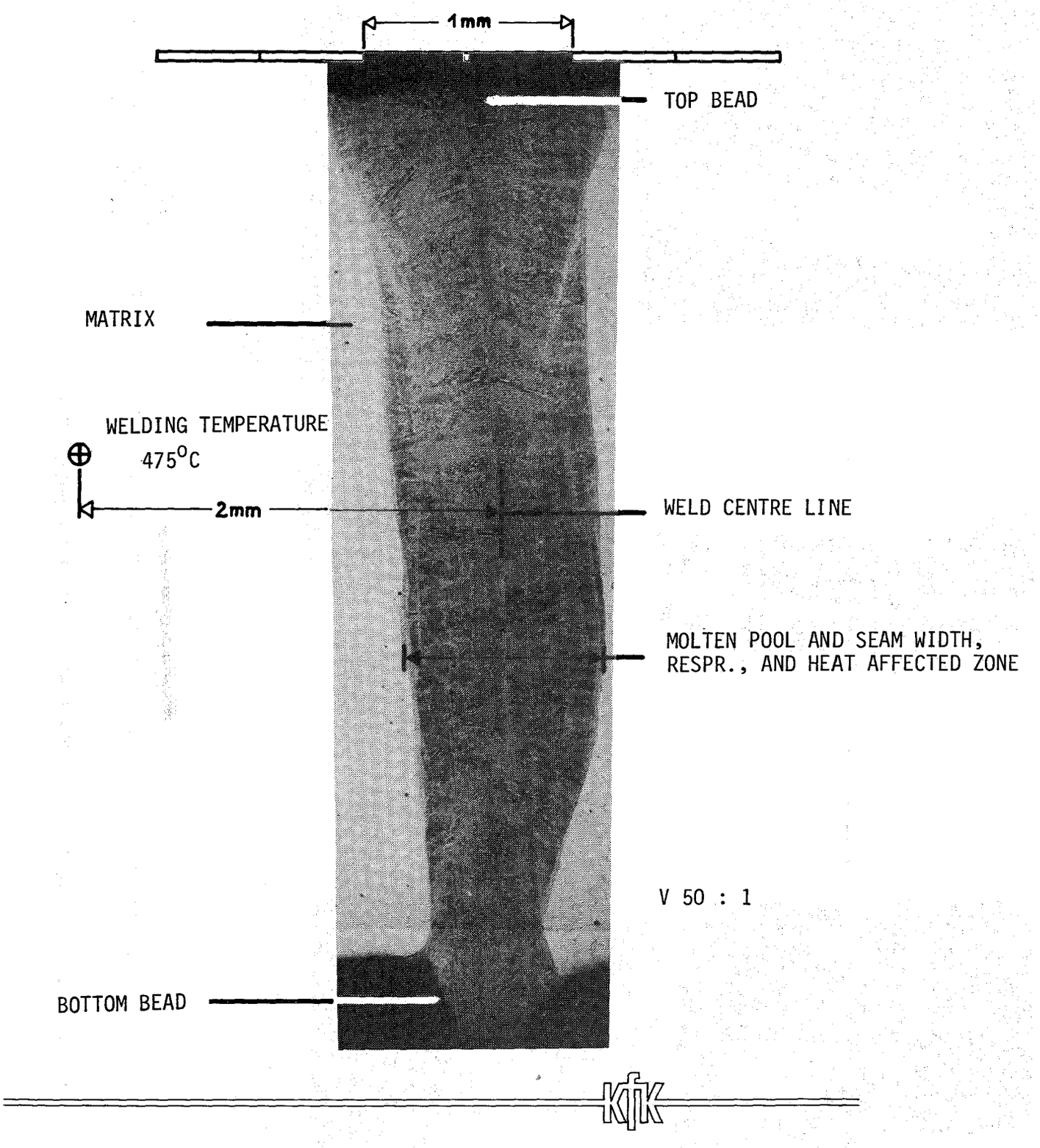

FIG. 14: TRANSVERSE MICROGRAPH OF AN ELECTRON BEAM WELDED HASTELLOY C4 SPECIMEN (IN SITU-TEST)

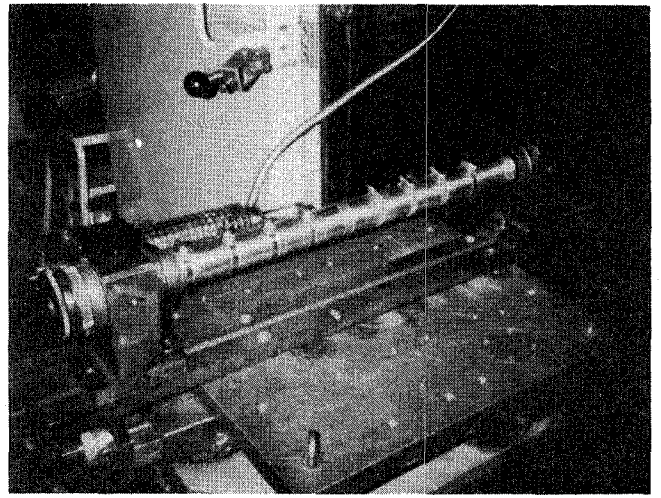

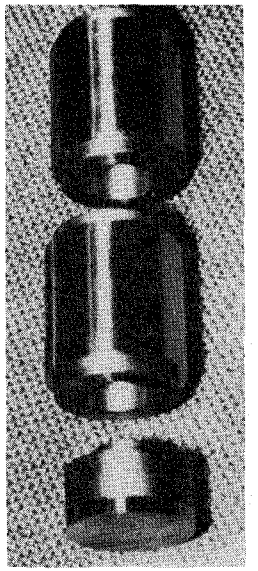

Parts of metal container

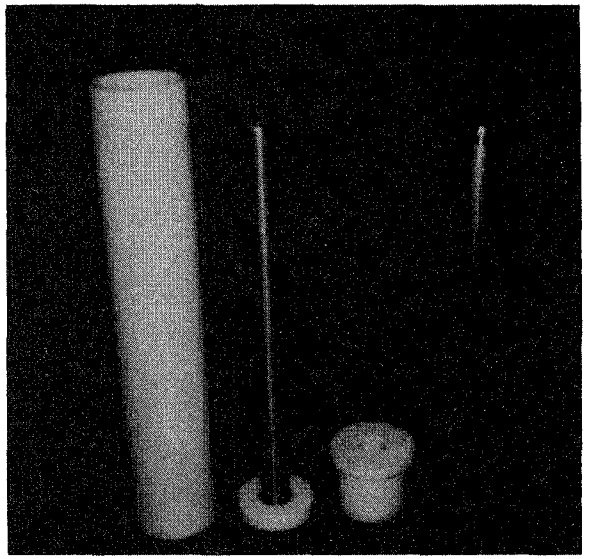

Parts of explosion plating

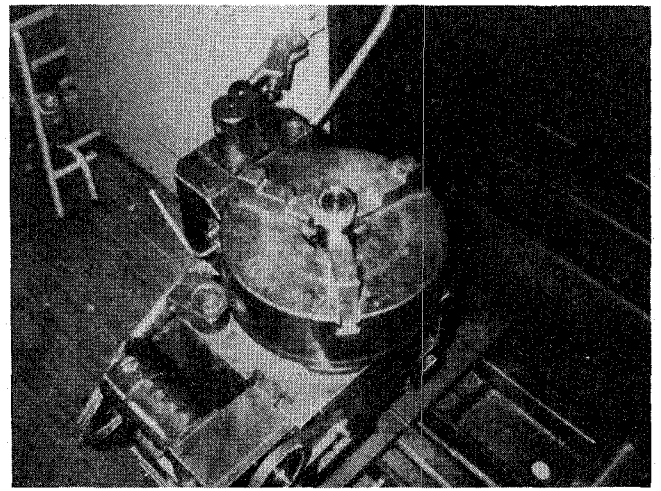

Simulation of the closing technique
by electron beam welding

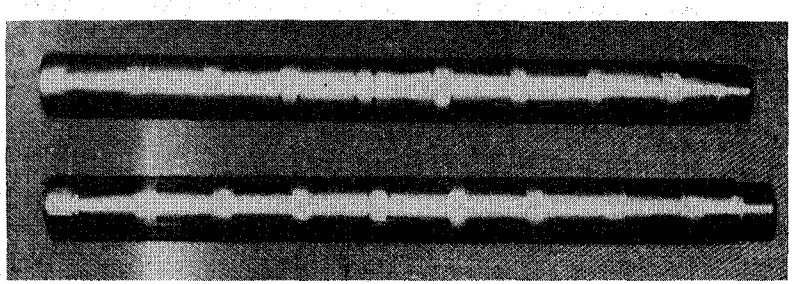

Model Container

FIG. 15: FABRICATION OF MODEL CONTAINERS (IN SITU-CORROSION TEST)

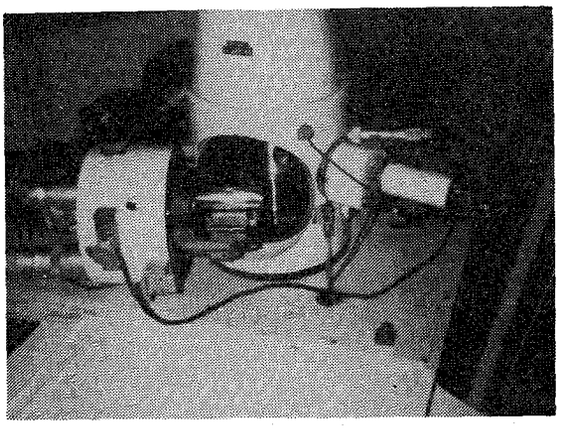

Part of plated and welded tube in SEM

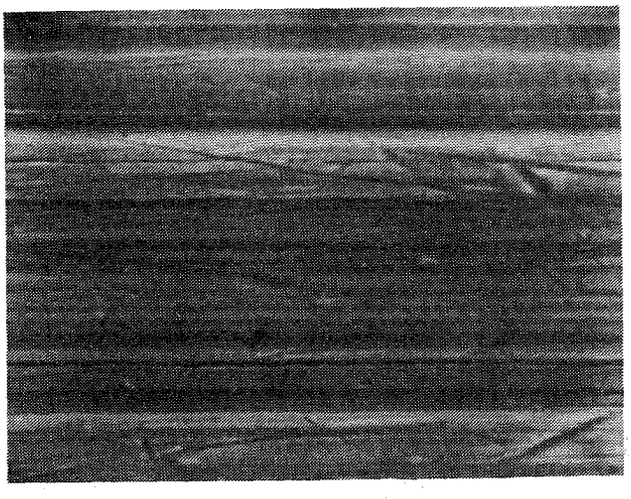

Tube surface

V 480:1

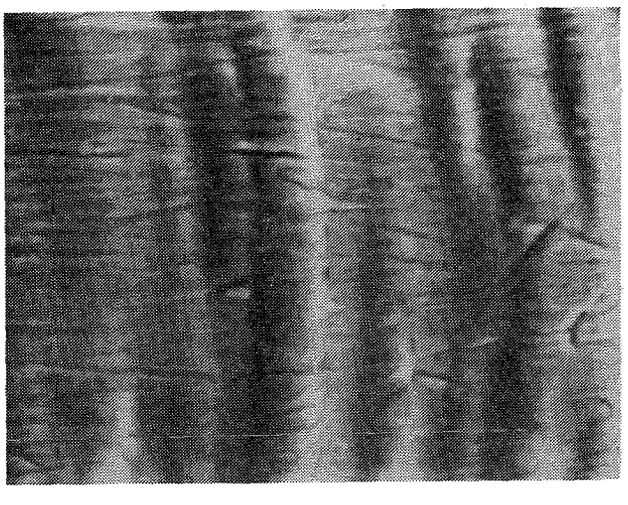

Weld surface

V 480:1

Fig. 16 SEM PHOTOGRAPHS OF SELECTED SITES OF THE TUBE SURFACE (IN SITU-CORROSION TEST)

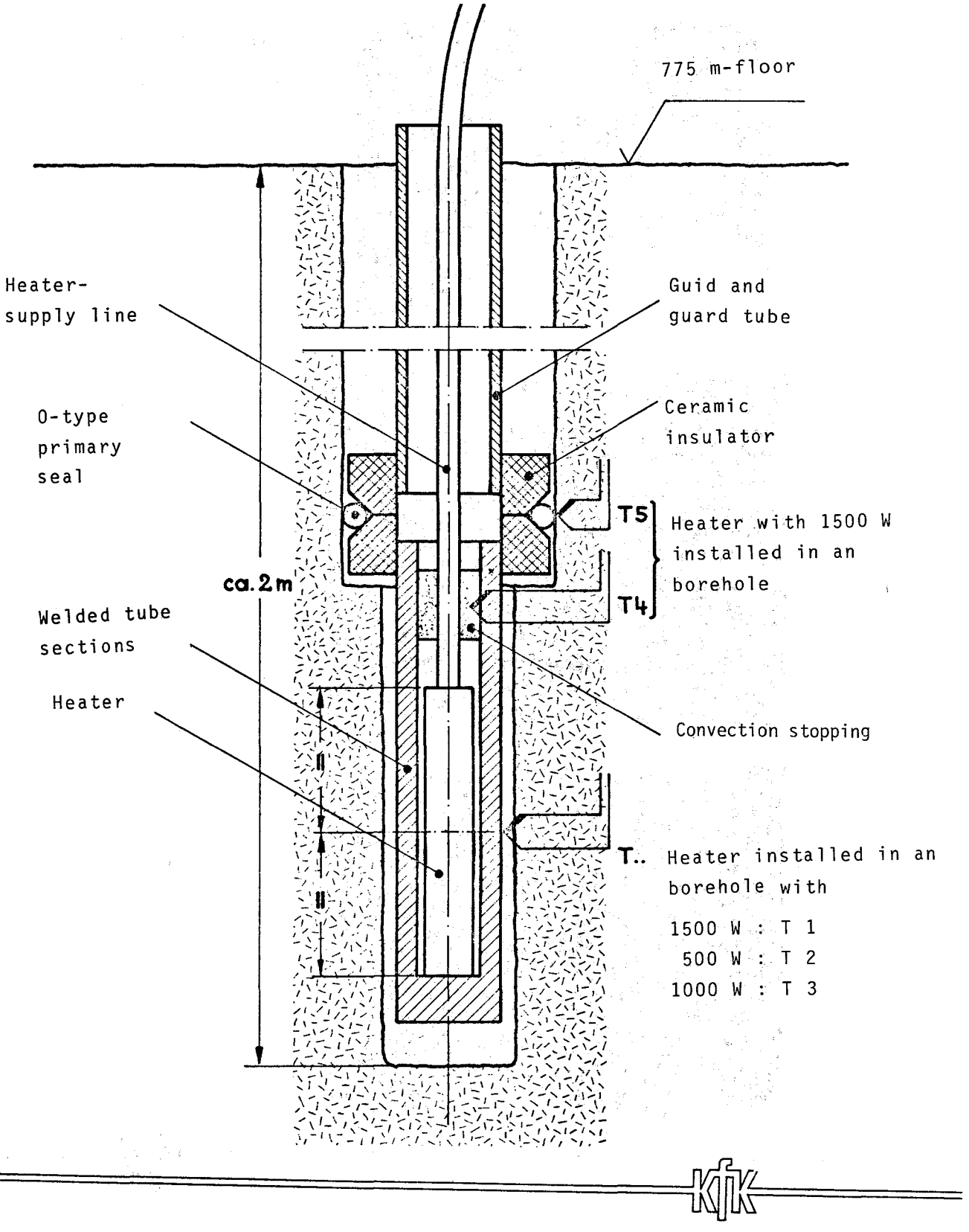

FIG. 17 Set-up of the preliminary in situ-test.

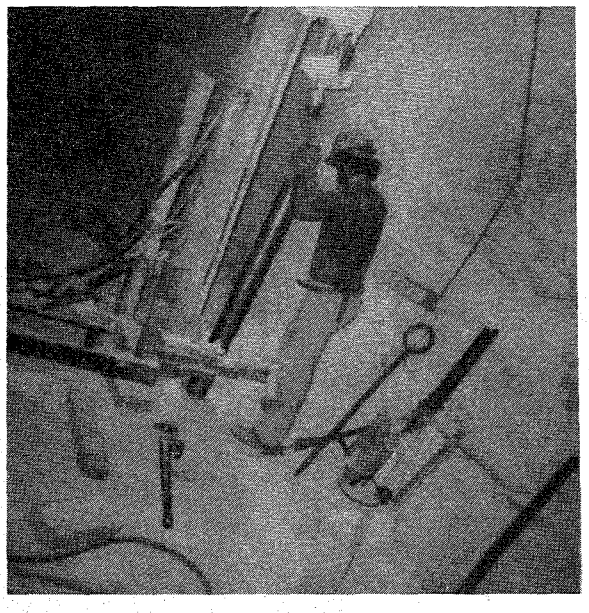

a) Core drilling technique for retrieval of the model containers

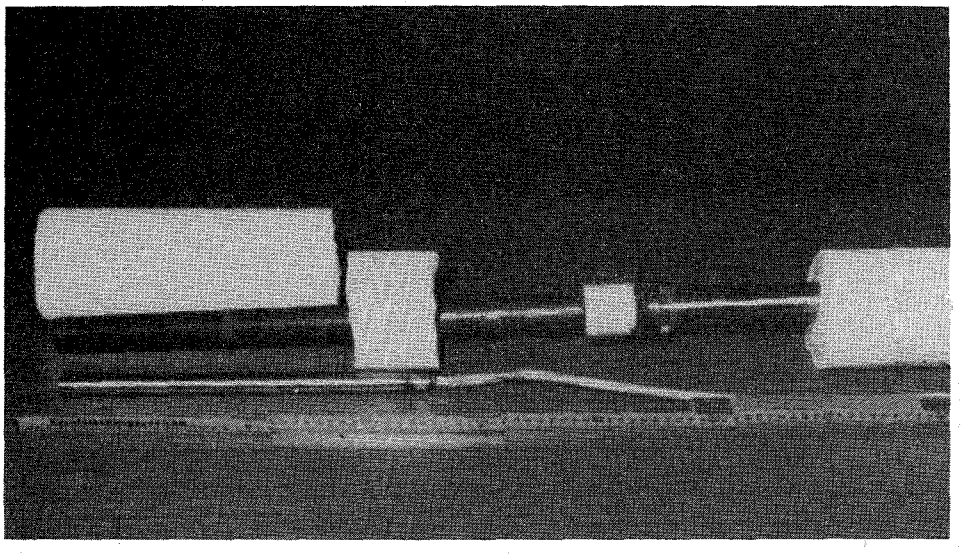

b) Retrieved model container with drill core and heating cartridge.

FIG. 18: IN SITU-INITIAL TEST

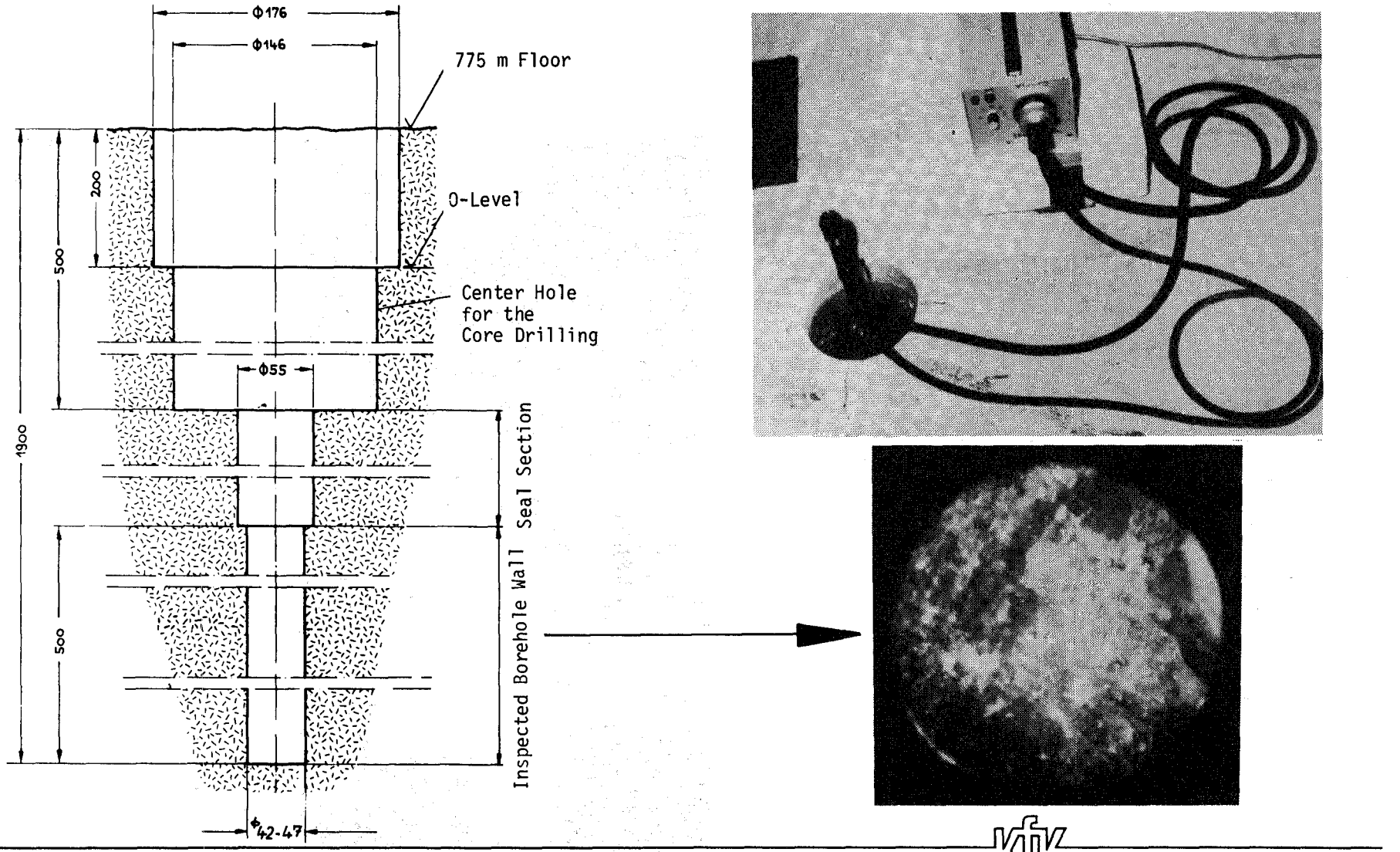

FIG. 19: BOREHOLE GEOMETRY AND ENDOSCOPE PHOTOGRAPH OF THE BOREHOLE WALL (IN SITU- CORROSION TEST)

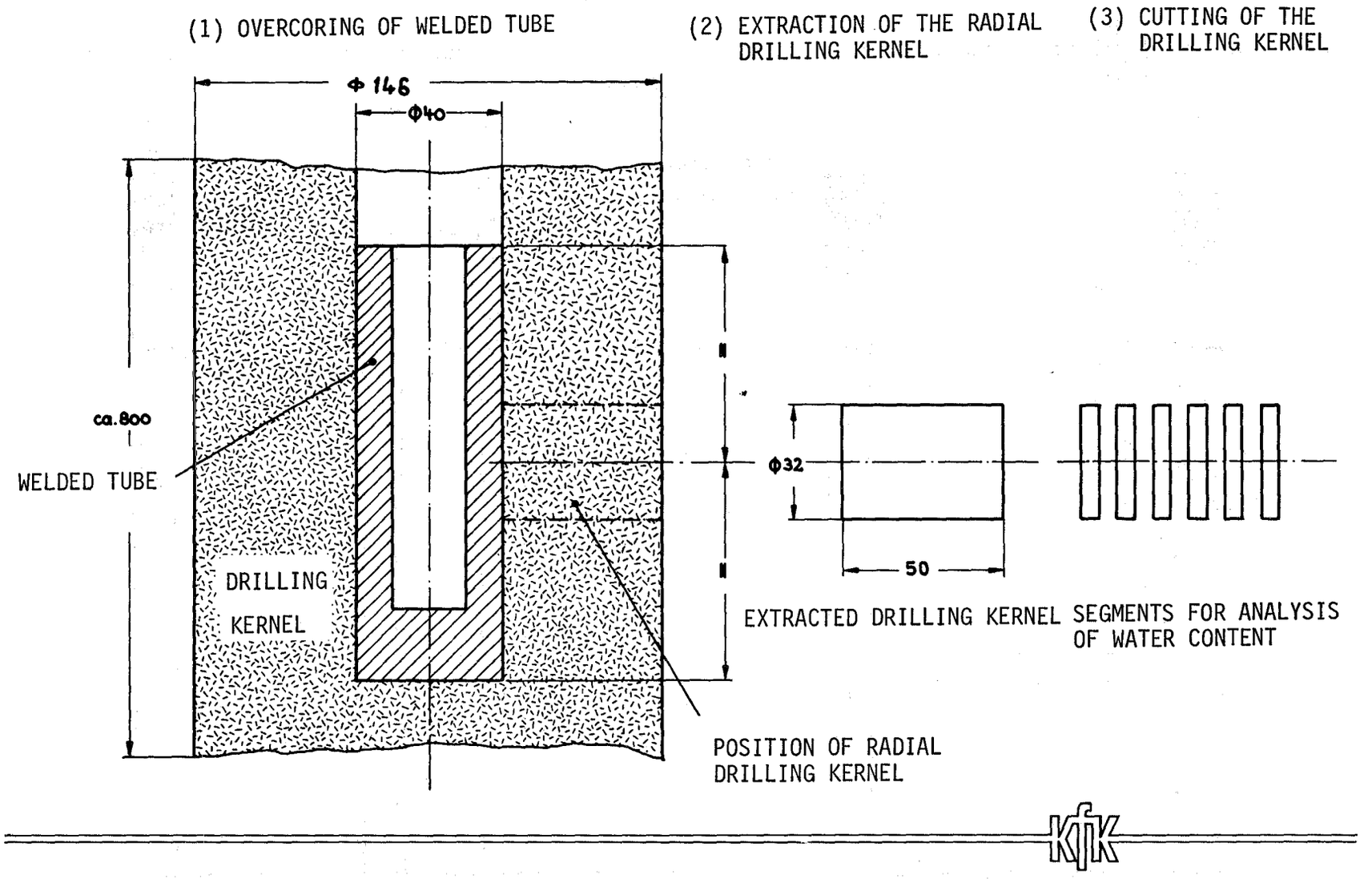

FIG. 20: SCHEMATIC OF WELDED TUBE AND DRILLING KERNEL WITHDRAWEL FOR POST EXAMINATIONS (IN SITU-CORROSION TEST)

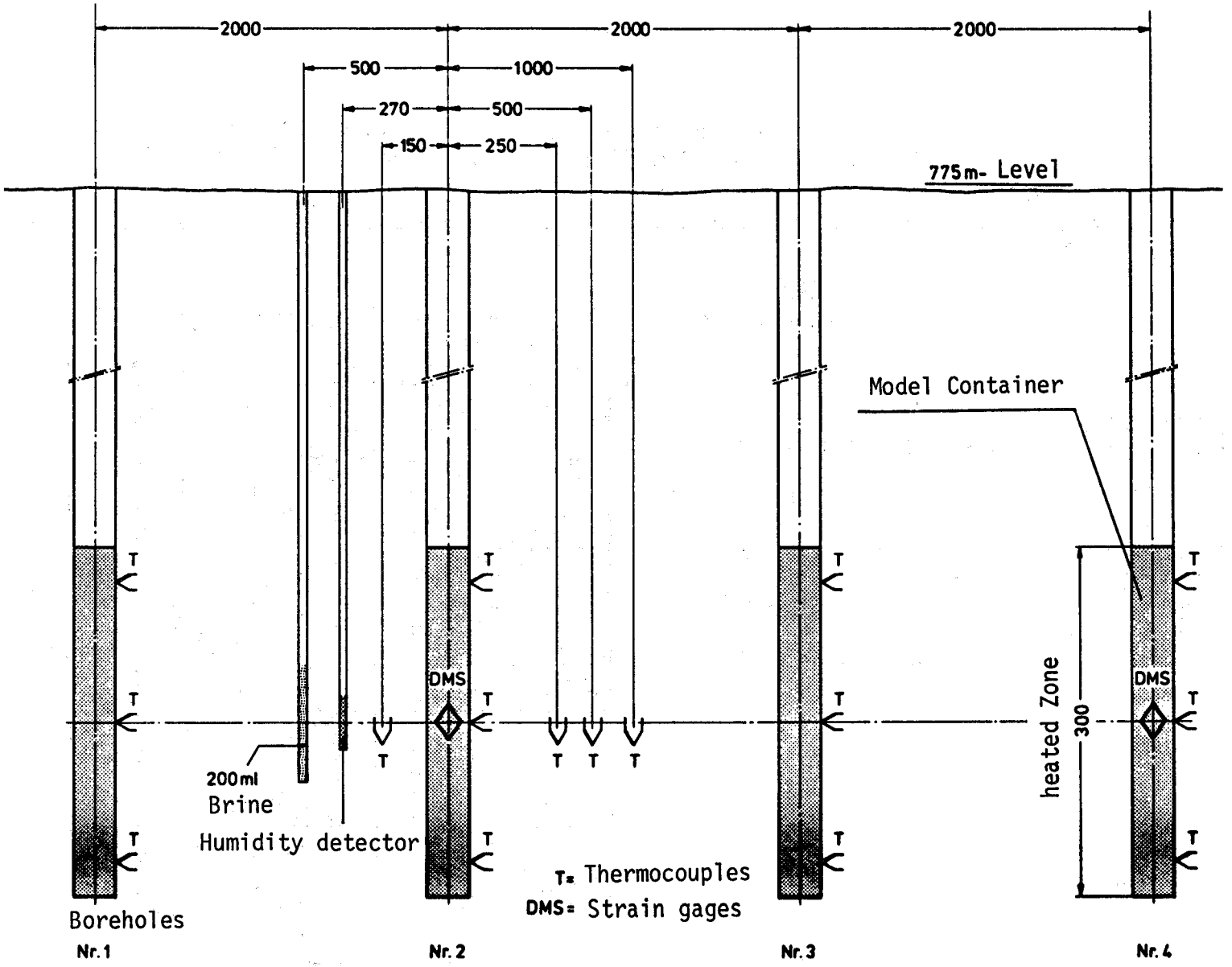

FIG. 21: MEASUREMENT EQUIPMENT OF THE IN SITU-TEST FIELD

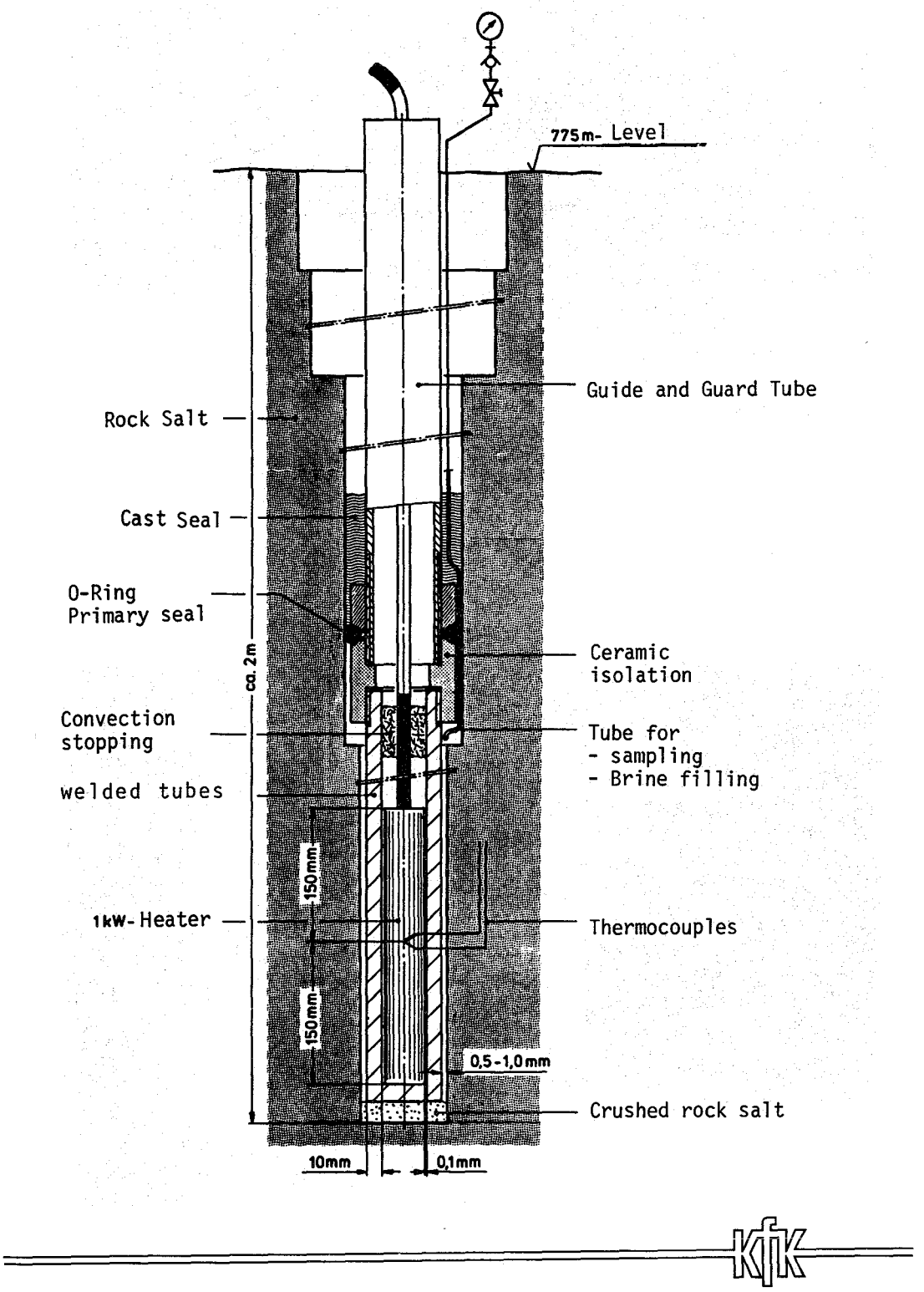

FIG. 22: SECTION THROUGH A STORAGE BOREHOLE
(IN SITU-CORROSION TEST)

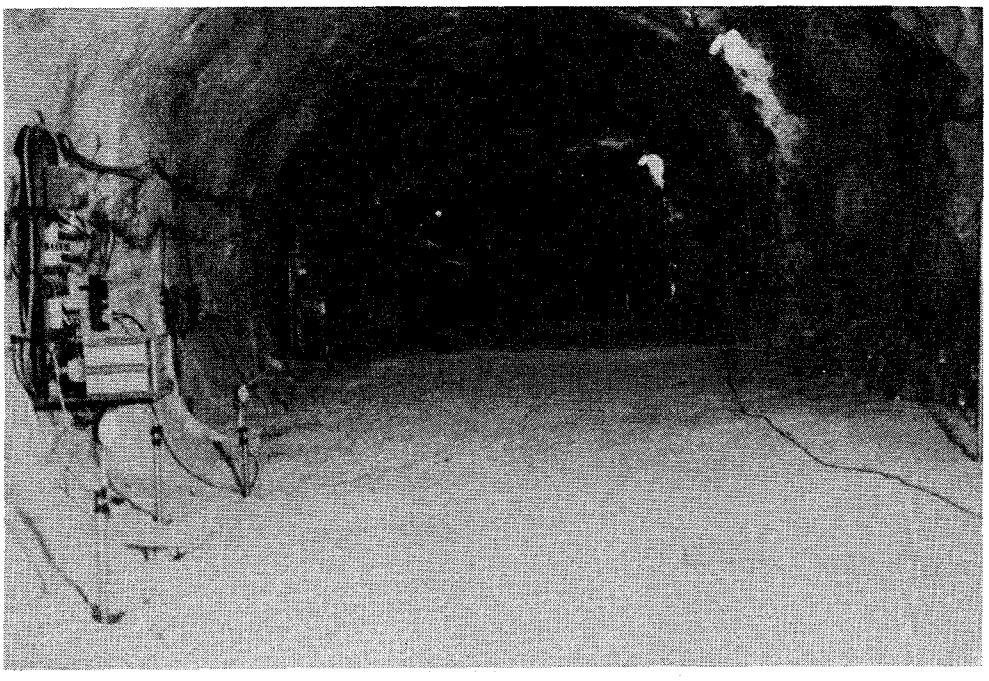

a) Overview

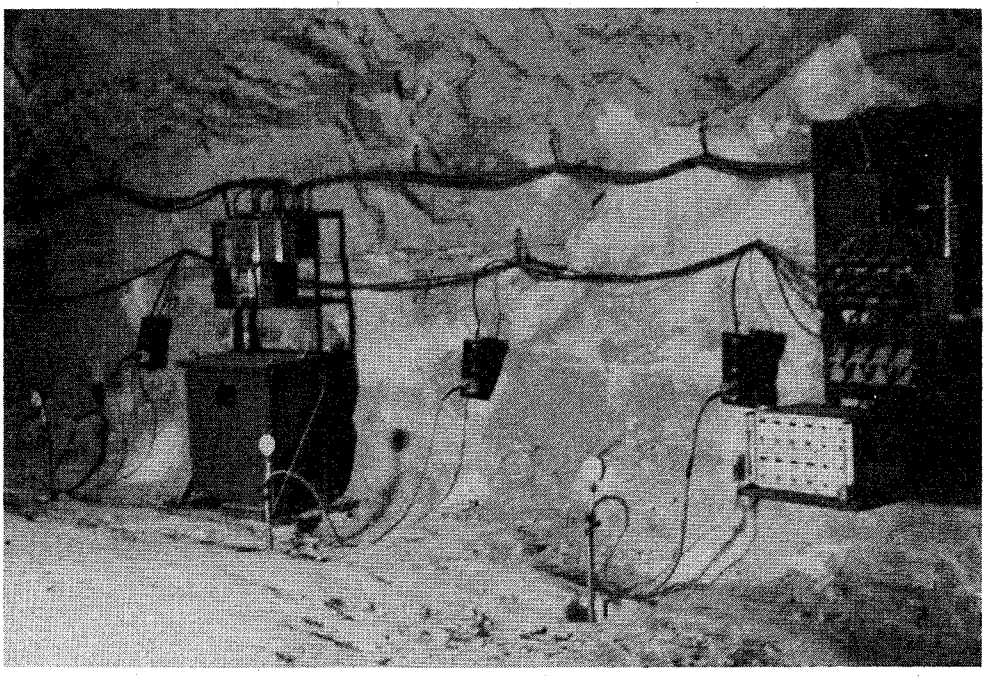

b) Power supply and temperature control of the heaters

FIG. 23: IN SITU-TEST FIELD

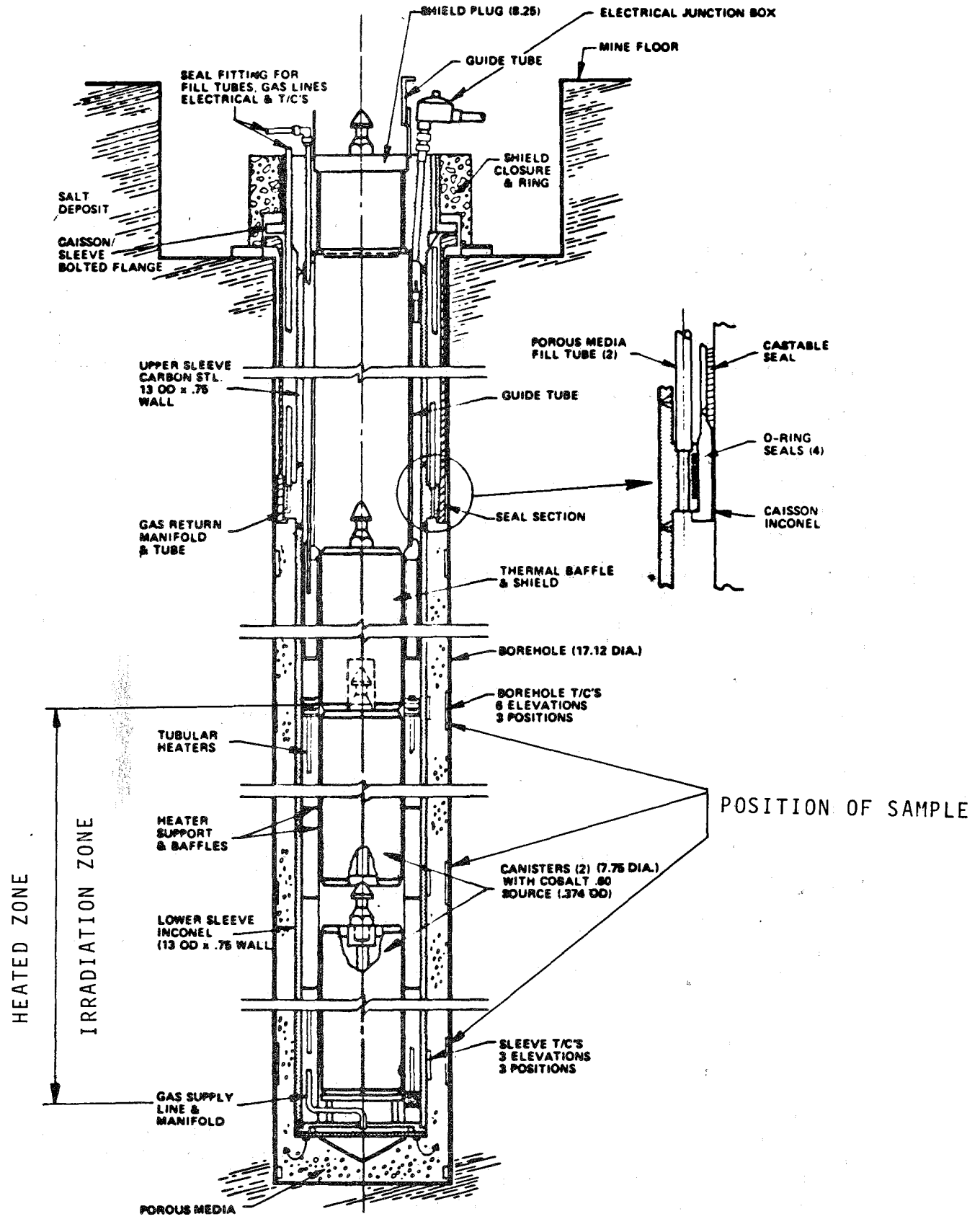

FIG. 24: CROSS SECTION OF BRINE MIGRATION TEST ASSEMBLY (IN SITU-CORROSION TEST)

4. Literature

/1/ E. Smailos, W. Stichel, R. Köster
Korrosionsuntersuchungen und mechanische Prüfungen an metallischen Werkstoffen zur Auslegung von Behältern für verglaste hochradioaktive Abfälle als Barriere im Endlager,
KfK 3230 (1981).

/2/ E. Smailos, B. Kienzler, R. Köster
HAW-Behälter als Barriere im Endlager, Proceedings of the International Seminar on Chemistry and Process Engineering of High Level Liquid Waste Solidification, R.Odoj, E. Merz (ed.), Jül-Conf-42, Vol. 2, pp. 926-953, (1981).

/3/ F. Canadillas, E. Smailos, R. Köster
Korrosionsuntersuchungen zur Eignung eines Baustahls für die Auslegung von Behältern zur Endlagerung hochradioaktiver Abfallprodukte,
KfK 3549 (1983).

/4/ E. Smailos, R. Köster, W. Schwarzkopf
Korrosionsuntersuchungen an Verpackungsmaterialien für hochaktive Abfälle,
EUR 8657, European Appl. Res. Rept. - Nucl. Sci. Technology, Vol. 5, No.2, pp. 175-222 (1983).

/5/ E. Smailos, W. Schwarzkopf, B. Fiehn, R. Köster
Corrosion Behaviour of Container Materials for Geological Disposal of High Level Wastes, Annual Progress Report 1983; EUR 9570, Part II, pp. 54-68 (1984).

/6/ R. Köster
Near Field Phenomena in Geological Repositories for Radioactive Wastes, Proceedings of an International Conference in Seattle, May 16-20, 1983, Radioactive Waste Management, Vol. 4, pp. 303-315 (1984).

/7/ R.E. Schmitt, F. Canadillas, R. Köster
Elektrochemische Untersuchung des Korrosionsverhaltens von Feinkornbaustahl 1.0566 und Weicheisen in chloridhaltigen, wäßrigen Lösungen,
KfK 3729 (1984).

/8/ Herbert H. Uhlig
Korrosion und Korrosionsschutz, Akademie-Verlag, Berlin (1970), S. 84 ff.

/9/ G. Pfennig, H. Moers. H. Klewe-Nebenius, G. Kirch, H.J. Ache
Surface Analytical Investigation of Corroded Ti 99.8-Pd Proposed as Container Material for the Disposal of High Level Wastes, Poster presented at International Conference on Nuclear and Radiochemistry, Lindau, Federal Republic of Germany, October 8-12, 1984.

/10/ Design Study on Containers for Geological Disposal of High-Level Radioactive Waste, from Ove Arup and Partners, Commission of the European Communities, EUR 9909 (1985).

/11/ N. Jockwer
Diss. Technische Universität Clausthal (1981).

/12/ E.S. Gaffney et al.
UCRL-15102 (1979).

/13/ W. Schwarzkopf
Im Ergebnisbericht über Forschungs- und Entwicklungsarbeiten 1982 des Instituts für Nukleare Entsorgungstechnik, KfK 3490 (1983), S. 34-35.

/14/ T. Rothfuchs
2. Halbjahresbericht 1981 der GSF, EG-Vertrag Nr. WAS 130-80-7 D, (unpublished).

/15/ T. Rothfuchs, K. Dürr
In situ-Investigation of Brine Migration Temperature Distribution and Convergence in Salt in a High-Level Waste Simulation Experiment at the Asse Salt Mine, HTD-Vol. 11.

/16/ J. Hengstenberg, B. Sturm, O. Winkler
Messen, Steuern und Regeln in der chemischen Technik, Springer-Verlag, Berlin, 1980, Band II, S. 161-205.

/17/ Westinghouse Electric Corporation
Brine Migration Test for Asse Mine, Federal Republic of Germany, Final Test Plan, ONWI-242 (1983).